RESEARCH ARTICLE

Geoarchaeology An International Journal WILEY

The role of geoarchaeology in the interpretation of fragmented buildings and occupation surfaces: The case of coastal settlements in northeast Scotland

Vanessa Reid[1] | Karen Milek[1] | Charlotte O'Brien[1] |
Óskar G. Sveinbjarnarson[2] | Gordon Noble[3]

[1]Department of Archaeology, Durham University, Durham, UK

[2]ECUS ltd, Barnard Castle, UK

[3]Department of Archaeology, University of Aberdeen, Aberdeen, UK

Correspondence
Vanessa Reid, Department of Archaeology, Durham University, Dawson Bldg., South Rd., Durham DH1 3LE, UK.
Email: vanessa.m.reid@durham.ac.uk

Scientific editing by Sarah Sherwood

Abstract

Around the world, poorly preserved buildings and occupation deposits often represent the primary evidence for archaeological structures and settlements. Integrated geoarchaeological methods, such as soil chemistry and micromorphology, can be used to maximise the information obtained from such deposits regarding site preservation and the use of space. However, archaeologists are often reluctant to apply these methods if they suspect that preservation is poor or stratigraphy is not visible in the field. To assess the role that geoarchaeology can play in the interpretation of fragmented and poorly preserved structures, this paper presents the results of two case studies in which multiple geoarchaeological methods (microrefuse analysis, pH, electrical conductivity, magnetic susceptibility, loss-on-ignition, portable XRF and micromorphology) were applied to poorly preserved occupation deposits and fragmented buildings in early medieval coastal settlements in northeast Scotland. Micromorphology proved to be fundamental for recognising and understanding the composition of occupation deposits that had formerly been floor surfaces. It also aided interpretations for the use of space and maintenance practices and improved an understanding of the post-depositional processes that had affected stratigraphic visibility at the macroscale. When subjected to principal component analysis, the geochemical, magnetic and microrefuse data were able to provide new details about activity areas, and successfully identified and filtered out the effects of post-medieval contamination. Most significantly, the integrated approach demonstrates that fragmented buildings and poorly preserved occupation surfaces can retain surviving characteristics of the use of space, even if the floor surfaces were not preserved well enough to be clearly defined in the field or in thin section.

KEYWORDS
geoarchaeology, micromorphology, preservation, settlement, site formation processes

Geoarchaeology. 2024;39:238–267.

1 | INTRODUCTION

Settlement remains are a vital resource for understanding the organisation and structure of past societies (e.g., LaMotta & Schiffer, 1999; Parker Pearson & Richards, 1994). Geoarchaeological investigation has been proven to be a particularly effective tool in characterising past human activity on settlement sites and providing detail on the rituals that governed everyday life (French, 2015; Jones et al., 2010; Milek & Roberts, 2013). However, archaeologists are often reluctant to apply these methods if they suspect that preservation is poor or stratigraphy is not visible in the field (Cannell, 2012; Goldberg, 1988, 2008; Goldberg & Aldeias, 2018; Macphail et al., 2003, p. 11). Underlying these decisions is the common assumption that little detail can be retrieved from poorly preserved structures and occupation deposits, and the vast majority of geoarchaeological case studies continue to be conducted on well-preserved sites with surviving structural elements and clear stratigraphic sequences (e.g., Borderie et al., 2020; Milek & Roberts, 2013). As a result, there has been comparatively little research on how integrated geoarchaeological methods can be used to improve the understanding of settlement sites that are poorly preserved and highly fragmented. This is despite the fact that geoarchaeological methods have transformed our understanding of severely bioturbated, homogeneous dark earths in European towns, providing information about activity areas and the formation processes that altered their original stratified deposits (e.g., Borderie et al., 2015; Devos et al., 2022; Wouters et al., 2019).

Equating thin, homogenised, fragmentary or truncated deposits with a paucity of evidence for settlement activity belies several fundamental principles of archaeological site formation. First, certain depositional events may not be apparent to the naked eye and their identification requires microscopic examination (Karkanas & Goldberg, 2016; Kühn et al., 2018; Lehmann & Schroth, 2003; Macphail & Goldberg, 2018, pp. 135–185). Second, there are multiple taphonomic factors that can modify the appearance of stratigraphy and affect the integrity of its microstructure and associated artefact and ecofact assemblages—although they do not necessarily result in the complete eradication of the original structure and composition (Huisman, 2009; Kibblewhite et al., 2015; Kooistra & Pulleman, 2018). Third, many residues of human activity are minute and only identifiable at a microscopic or molecular scale (Sulas et al., 2022; Weiner, 2010). Omitting their analysis is therefore likely to result in key evidence of settlement character being overlooked and the creation of less detailed and less reliable interpretations of archaeological structures and their assemblages.

To overcome this, numerous geoarchaeological techniques can be used to study the residues left behind by humans and animals. Soil micromorphology has been proven to be the gold standard in resolving microstratigraphic detail and understanding the composition, preservation and post-depositional alteration of archaeological deposits (Banerjea et al., 2015; Courty et al., 1989; Lewis, 2023; Robertson & Roy, 2021). Geochemical assessments—such as pH, organic matter content and multi-element analysis—can provide corroborating evidence

of burial conditions and aid the interpretation of activity areas (Borderie et al., 2020; Milek et al., 2023; Nielsen & Kristiansen, 2014; Wilson et al., 2008). These techniques have been shown to be particularly effective when integrated into multi-method data sets (Jones et al., 2010; Kidder et al., 2021; Mentzer & Quade, 2013; Milek & Roberts, 2013; Reidsma et al., 2021; Shillito, 2017; Sulas et al., 2022).

To assess the effectiveness of geoarchaeological methods in elucidating formation processes and the use of space in fragmented buildings, this paper presents two case studies in a geographic area where preservation has previously limited interpretations of archaeological settlement remains. Poorly preserved buildings and occupation surfaces are a common feature of early medieval settlement in northeast Scotland, where secure traces of structural elements and internal deposits are often absent, heavily fragmented or poorly defined (Driscoll, 2011; Dunwell & Ralston, 2008, pp. 133–140; Reid, 2021; Reid & Milek, 2021). Ephemeral building traditions and the use of none-arthfast materials appear to be contributing factors, and features are commonly truncated through later agriculture, urban development, coastal erosion or stone robbing (Dunwell & Ralston, 2008, p. 140; Noble et al., 2020, p. 320; Reid & Milek, 2021). The lack of structural remains is typically accompanied by a poor volume of finds and has been exacerbated by a tendency towards small scales of excavation. Very little geoarchaeological investigation has been conducted in the region and the paucity of evidence has resulted in several cases where clarifying function, status or date has proved almost impossible (e.g., Driscoll, 1997; McGill, 2004; Noble et al., 2019, p. 84).

Excavations conducted by the University of Aberdeen's 'Northern Picts' project provided an opportunity to apply integrated geoarchaeological methods to two poorly preserved buildings on the eastern Scottish coast (Figure 1). Investigations at Burghead and Dunnicaer coastal promontory forts established the potential survival of fragmented floor layers within partial structures, whose architectural elements had been truncated, degraded or lost to erosion. Dedicated geoarchaeological sampling strategies were used to investigate the integrity of these floor deposits and whether they retained any micro-evidence of site activity. The distributions of microrefuse and geochemical properties—pH, soluble salt content (electrical conductivity), organic matter (loss-on-ignition), magnetic susceptibility and multiple elements—were subjected to principal component analysis (PCA), mapped across the excavated surfaces and compared against the results of micromorphological analysis. The intention was to improve our understanding of the type of micro-information retained in fragmented buildings and occupation surfaces and expand the toolbox that archaeologists use to refine interpretations.

2 | STUDY AREA

2.1 | Burghead

Situated on a peninsula that projects northwest into the Moray Firth, Burghead Fort (NRHE No. 16146; NJ 1090 6914) is one of

FIGURE 1 Composite image of Burghead (left) and Dunnicaer (right) study sites showing (a) location of study sites in relation to Scotland; (b) oblique aerial image of Burghead looking south-east with 2017 excavation trenches; (c) location of 2015–2017 Burghead excavation trenches in relation to Burghead town and Pictish ramparts; (d) location of Dunnicaer sea stack on Aberdeenshire coast; and (e) aerial drone image of Dunnicaer sea stack during 2017 excavations, showing extensive erosion at the north-east end and location of lower terrace excavations (photographs © Gordon Noble; diagram [c] adapted from Noble et al. [2018]; contains OS Data © Crown copyright and database right 2022; © University of Aberdeen).

the largest and most impressive Pictish settlements currently known (Foster, 2014, p. 46; Noble, 2019, p. 46) (Figure 1). It is situated in an area of sandstone outcrops, with overlying marine deposits of gravel, sand and silt. The soils in the vicinity of the site are classified as noncalcareous regosols (well-drained, immature soils developed on windblown sands); however, the soils at the site itself are classified simply as 'built up land' (Soil Survey of Scotland Staff, 1981). All original soils at the site were truncated and/or buried by the construction of the Pictish fort and an overlying 19th-century village.

The fort covered an area of around 5.5 ha, with stone ramparts defining an upper and lower citadel (Alcock, 2003, pp. 192–197; BGS, 2022; Foster, 2014, p. 47). Archaeological evidence and radiocarbon dates suggest that the fort was occupied since at least the 6th century A.D. and was destroyed by fire in the 9th or 10th century (Noble & Evans, 2022, p. 111).

Much of the fort was lost during the construction of the planned village and harbour in the 19th century, which revealed a deep well and up to 30 Class I symbol stones carved with bull imagery (Oram, 2007). These monuments, and the immense size and complexity of the fort, all indicate that Burghead was a major Pictish power centre during the first millennium A.D.

Excavations by the Department of Archaeology, University of Aberdeen, have been ongoing since 2015 and are adding considerable detail to an existing corpus of work on the site (Edwards & Ralston, 1978; Macdonald, 1862; Ralston, 2006; Small, 1969; Young, 1891, 1893). They have so far identified evidence of structures in both the upper and lower citadels, revealed complex timber-laced ramparts and recovered a wealth of artefacts including coins, iron weaponry and carved bone pins. Parts of the site have already been undermined by coastal erosion, and recent excavation seasons have been conducted as part of a Historic Environment

Scotland-funded programme intended to capture as much information as possible before it is lost to the sea.

The 2015–2017 excavation seasons explored the extent and nature of Building 2—a subrectangular structure in the upper citadel that measured at least 8 m in length and 5 m in width (Figures 2 and 3). It lay below a layer of light brown sand and gravel that was attributed to landscaping of a modern garden and contained a large amount of 19th–20th century midden material. A highly fragmented turf and stone wall survived only in the northwest end and measured up to 0.3 m in height, 0.7 m in width and 4.0 m in length (Figure 2a). This part of the structure contained a hearth made of flat flagstones (heavily robbed) and a thin deposit (context 17,040—max. 0.1 m thick) of fine, dark grey sand interpreted as a floor layer (Figure 3). A charcoal-rich deposit (17,039) containing burnt oak timbers overlay this occupation surface at the northwest end and was interpreted as the remains of a timber superstructure that may have been destroyed by fire. Finds included an iron buckle, an iron sword hilt, a 9th-century pierced Anglo-Saxon coin and a broken rotary quern.

Preservation became increasingly poor towards the southeast end of the structure, where the turf wall no longer survived. Two deposits—a black sand (105) and an underlying sand containing charcoal (106)—were interpreted as occupation surfaces based on their colour, compacted nature and number of postholes that were situated within the layers or just underneath them. Context 106 was considered a possible extension of context 17,040 (Figures 2b and 3); however, the extent of both 105 and 106 became unclear towards the southeast end of the trench, where 19th-century ceramics, postholes, a stone wall and industrial waste consisting of coal, clinker, cinder and slag were discovered. This indicated that 19th-century activity had penetrated the early medieval layers and had likely truncated or contaminated archaeological deposits in the southern edges of the trench. Radiocarbon dating of the lower surface (106) placed activity in the 9th–10th century A.D.; however, no dating material was retrieved from 105. A concentration of postholes in the east of the 2016 trench was radiocarbon dated to the 7th–8th centuries A.D. and a shallow ring-ditch underlay the lower floor of Building 2, suggesting that there had been an earlier structure.
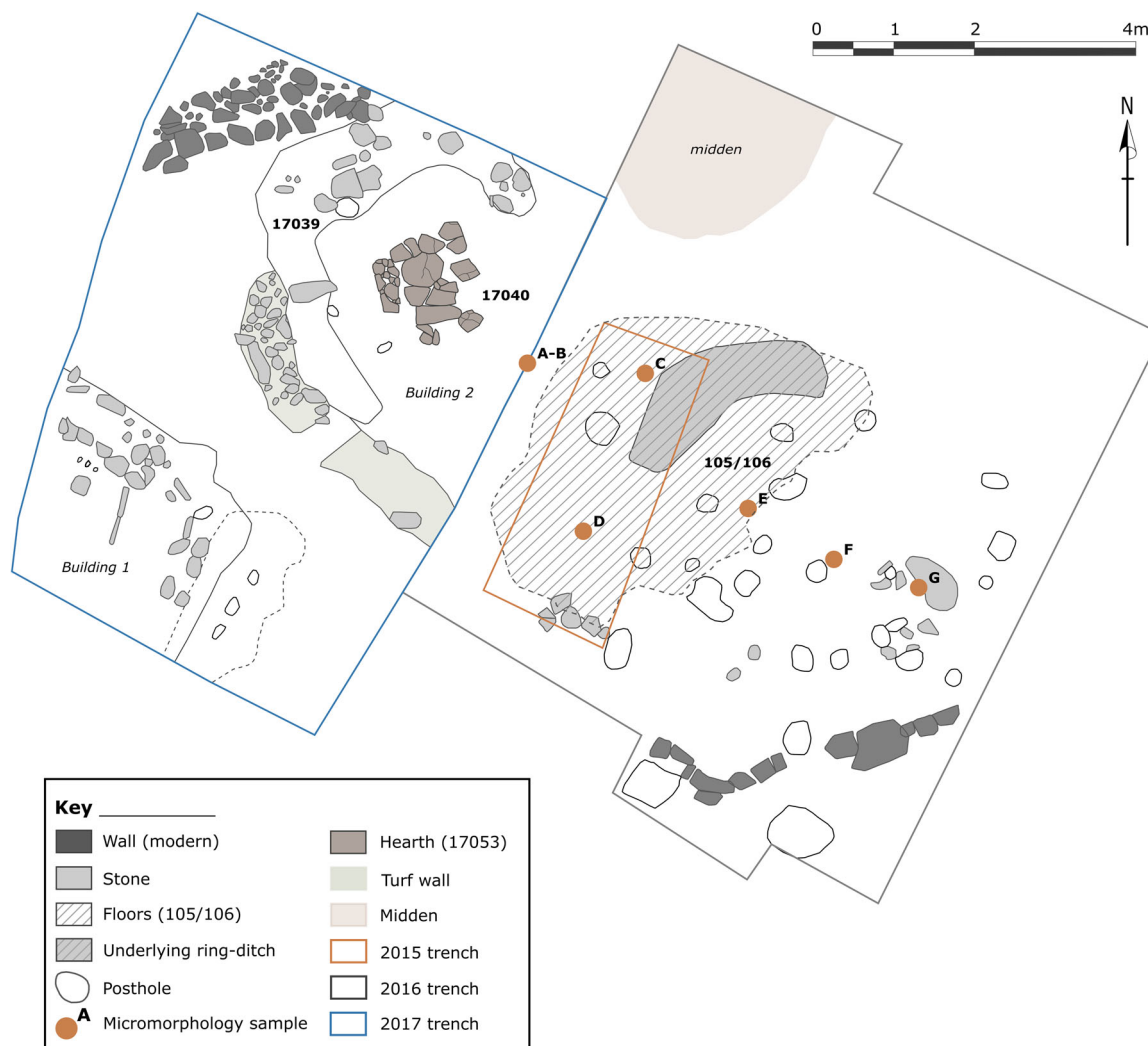
2.2 | Dunnicaer

Dunnicaer (NRHE No. 37001; NO 8821 8464) is a severely eroded sea stack on the Aberdeenshire coast, just south of the town of Stonehaven (Figure 1). The stack is composed of conglomerate rock with sandstone veins and stands to a height of 21 m. It measures 54 m long and up to 20 m wide, with the top divided into an upper terrace (max. 24 × 14 m) and a smaller lower terrace (max. 8 × 8 m) (Noble et al., 2020, p. 265). Soils in the immediate vicinity are classified as imperfectly drained brown soil (Soil Survey of Scotland Staff, 1981) but on the site itself these were truncated by occupation activity and 19th-century stone quarrying and cultivation on the upper terrace. Deposits from the upper terrace had slumped into the lower terrace and consisted of a very loose overburden of small stones and organic humic-rich soils. Below these slumped layers was an in situ midden layer, up to 0.1 m thick, of organic-rich soil with abundant charcoal and a few small fragments of poorly preserved animal bone (Noble et al., 2020, p. 283). Five Pictish symbol stones were recovered from the stack during the 19th century, and excavations by the University of Aberdeen (2015–2017) revealed the remains of a highly eroded promontory fort dated to the Roman Iron Age (1st–4th centuries A.D.). Evidence included the remains of a timber-laced or framed rampart, multiple hearths, occupation deposits, imported Roman Samian and coarse-ware, and burnishing stones for metalworking.

FIGURE 2 Drone images of Building 2 at Burghead showing (a) final excavation of the 2017 trench with hearth (17,053) and turf/stone wall and (b) mid-excavation of the 2016 trench with occupation deposit (105/106) and 2015 baulk (photographs © Óskar G. Sveinbjarnarson).

FIGURE 3 Final excavation plan of Building 2 at Burghead showing deposit context numbers, hearth and location of micromorphology samples.


FIGURE 4 Oblique view of the lower terrace trench at Dunnicaer looking north-east, showing the floor (1009), charcoal spread (1007) and upper hearth (1008) immediately before bulk sampling (photograph © Gordon Noble).

Results of the excavation, specialist reports and contextual analysis were published in Noble et al. (2020).

In 2016, excavation exposed deposits and settlement features on the lower terrace. Occupation evidence consisted of two overlying subrectangular stone hearths associated with 0.3 m of compacted floor deposits (1009) and a hard-packed deposit of redeposited natural sediments that may have functioned as a levelling surface. The stones of the lower hearth (1012) were significantly more fire-cracked than those that made up the upper hearth (1008), indicating intensive and perhaps long-lived use of this feature. To the west of the upper hearth, a distinct charcoal-rich deposit (1007) was interpreted as probable ash rake-out (Figures 4 and 5). Despite the fact that preservation was more favourable in the lower terrace due to the slumping of deposits and the lack of 19th-century stone quarrying and cultivation that had truncated features in the upper terrace, there were no obvious postholes or outer walling associated with the hearths, implying that the main structural elements had been lost to erosion or lay outside the limits of the trench (Noble et al., 2020, p. 319). There was no evidence for destruction by fire, and the structure and fort are believed to have been abandoned around the beginning of the 5th century A.D. (Noble et al., 2020, p. 330).
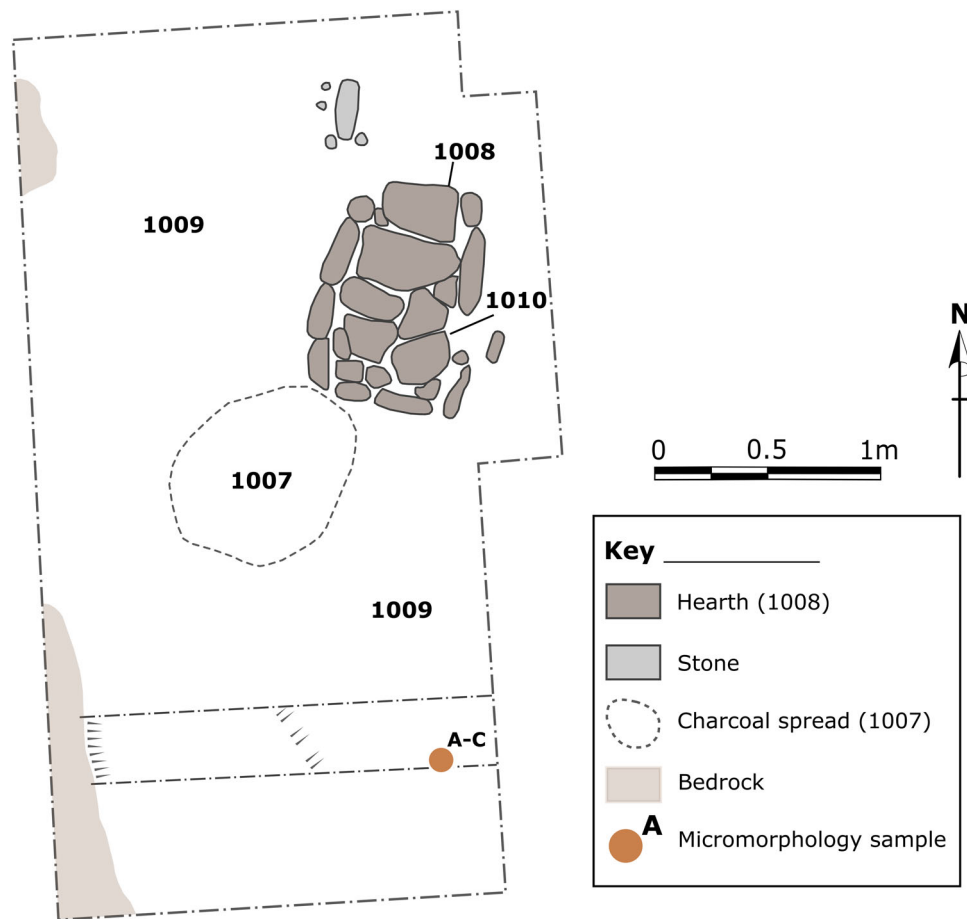
FIGURE 5 Mid-excavation plan of the lower terrace trench at Dunnicaer showing the location of micromorphology samples, context numbers, upper hearth and charcoal spread exposed at the time of sampling.

3 | METHODS

3.1 | Sampling

Occupation deposits at both sites were recorded and sampled using a 0.5 m grid during the 2016 excavation season. Small bulk samples (c. 200 mL) for geochemical, microrefuse and magnetic analyses were collected by hand from each grid square and given a unique identifier. At Burghead, bulk sampling concentrated on the two overlying occupation deposits believed to be floor layers to assess their nature and extent, and map post-depositional contamination (Figure 3). The upper sampling grid (*n* = 96) captured layer 105, and the lower sampling grid (*n* = 131) captured layer 106. These layers were clearly discerned on the basis of their black colour and higher compaction; however, they became hard to trace towards the eastern end of the trench. The sampling grid was therefore extended to determine the character of the western side of the trench and whether it related to these darker deposits (Figure 12). At Dunnicaer, bulk sampling was aimed at characterising activity surrounding the upper hearth. This occurred on a smaller scale (*n* = 24) owing to the limited space available in the lower terrace (Figure 5). Given the extent of urban development at Burghead, and Dunnicaer's location amidst

agricultural land, it was not possible to source nearby control samples with 'natural' background levels of magnetic susceptibility, pH or elements. Investigations have therefore been conducted with regard to intrasite variability.

A total of 10 undisturbed block samples (Burghead *n* = 7; Dunnicaer *n* = 3) were taken for micromorphological analysis from exposed sections in the baulks and edges of the excavations (following Courty et al., 1989). The block samples targeted visible occupation deposits and at Burghead also involved collecting samples on the eastern side of the trench, where the occupation deposits were less clear, in the hopes that micromorphological analysis would help clarify the spatial extent of the deposits (block locations and section drawings are provided in File S1).

3.2 | Sediment processing and analysis

Bulk samples were air-dried, gently powdered with a mortar and pestle and sieved through 2 mm mesh. The fraction above 2 mm was sorted by hand and examined for microrefuse such as charcoal and burnt bone, and the fraction below 2 mm was used for sedimentary analyses (Rowell, 1994). As bulk volumes varied, standardised

microrefuse values for a 200 mL sample were calculated. Selected microrefuse results are discussed and presented within the geo-chemical data (Sections 4.1.2, 4.2.2 and and 4.4); additional values can be found in Files S2–S4.

Electrical conductivity (EC) and pH were tested using a Hanna HI98130 metre immersed in a 10:20 mL soil:deionised water suspension. Organic matter content was estimated via loss-on-ignition (LOI) at 550°C for 3 h. Magnetic susceptibility was tested in 10 mL plastic pots using a Bartington MS3 magnetic susceptibility metre with an MS2B dual frequency sensor using the low-frequency setting (Dearing, 1999).

Element concentration determination was performed by portable XRF (pXRF) spectrometry on pressed pellets using a bench-mounted portable X-ray fluorescence analyser (NITON XL3t-Goldd+; Thermo Scientific). Sediment pellets of 10 mm depth were prepared by pressing air-dried and 2 mm sieved bulk samples to a pressure of 11 Tons using a Perkin–Elmer press. The equipment was operated in Cu/Zn mining mode and the instrument was configured to run for 60 s per sample. Using proprietary software, elemental concentrations were calculated using a fundamental parameters calibration. The instrument was internally calibrated on each start up and tested against NIST standards to check for contamination. Five replicate measurements were taken for each pellet and the mean value was accepted as representative of the grid square. Elements that returned values within the limits of detection were subjected to multivariate statistical analyses (see Section 3.3). As missing data can affect the validity of statistical analysis, grid squares with element concentrations below the limit of detection (<LOD) were substituted with LOD/2 in accordance with Farnham et al. (2002). Elements whose < LOD values exceeded 25% of the replicates were excluded from statistical investigation (Farnham et al., 2002). The remaining suite of elements comprised Al, Ba, Ca, Cr, Fe, K, P, Rb, S, Si, Sr, Ti and Zr. Complete geochemical data sets, including grid coordinates, are provided in Files S2–S4.

Soil and sediment thin sections were prepared following the University of Stirling's (2008) Thin Section Micromorphology Laboratory's standard procedures. All samples were dried using vapour-phase acetone exchange and impregnated with crystic polyester resin under vacuum, before being cut and precision lapped to 30 μm. Slides were scanned using a high-resolution flatbed scanner and initial assessment of the thin sections was conducted at a 1:1 scale on a lightbox. Microscopic observations were made using Leica M80 and Leica DM2700 P microscopes at a range of magnifications from ×4 to ×400 with plane-polarised light (PPL), oblique incident light (OIL) and cross-polarised light (XPL). Thin-section descriptions were conducted using the identification and quantification criteria set out by Bullock et al. (1985) and Stoops (2021), with reference to additional texts including Nicosia and Stoops (2017), Stoops et al. (2018) and Fitzpatrick (1984).

3.3 | Statistics, multivariate data analysis and data presentation

Statistical analyses of all variables (excluding microrefuse) were conducted using IBM SPSS and OriginLab Origin Pro to examine the distributions of data, correlations between different element concentrations and correlations between element and geochemical results. Shapiro–Wilk tests of normality indicated that multiple variables within the Burghead data sets were not normally distributed. However, as both had $n > 30$, the central limit theorem could be applied in which normality is assumed when sample sets have a high number of data points (Kwak & Kim, 2017). As the variables were measured in different scales, standardisation (z-score) was performed before multivariate analysis to ensure that each one contributed equally. Outliers were included in the data analysis as they were deemed to show variability of the sediments assessed (following Gardner, 2018).

PCA was performed to examine the overall structure of the data sets, and the results were interpolated in ArcMap 10.8.2 by ordinary kriging using a spherical semivariogram model to provide a more visual representation of the data. Interpolated surfaces were compared against distribution maps of the microrefuse and geo-chemical data sets to corroborate results and inform interpretations. Where applicable, distribution maps of additional elements (Cl, Cu, Ni, Pb, V and Zn) excluded from statistical analysis were also generated. Graduated symbols in equal intervals were chosen to represent the individual variables, as interpolation of these was not possible between different contexts and across walls. Burghead's upper surface was represented by graduated symbols in natural breaks (Jenks) as contamination in part of the trench had elevated elemental values to such an extent that more nuanced signatures in archaeological deposits were masked by equal interval mapping. The Dunnicaer sample size of 24 was too small for reliable PCA (see Shaukat et al., 2016), so data were interrogated by the visual comparison of these maps and the results of Spearman's rank correlation coefficient (r_s) for nonparametric data. For each of the sites, selected variables have been chosen for visual presentation due to their contribution to the interpretation of activity areas and taphonomic processes. Mapping of the additional variables is provided in Files S2–S4.

4 | RESULTS

## 4.1 | Burghead upper surface (containing 105)

4.1.1 | PCA results

PCA analysis of the geochemical results from Burghead's upper occupation deposit revealed three principal components (PCs) that met the Kaiser criterion (Kaiser, 1960, 1970) and accounted for 79.79% of the total variance (Table 1).

The first principal component (PC1) accounted for 66.21% of the total variance and appeared to reflect areas with a higher organic content and a lower mineral component, demonstrating high positive loadings (>0.75) for 12 of the 17 variables (EC, LOI, magnetic susceptibility, Al, Ca, Cr, Fe, P, S, Sr, Ti, Zr) and high negative loadings (>−0.80) for Si and K (Figure 6).

TABLE 1 Results of the first three principal components for Burghead upper surface, showing loadings and % of the variance explained.

Components	PC1	PC2	PC3
pH	−0.39	0.73	−0.41
Electrical conductivity	0.81	−0.25	0.31
Loss-on-ignition	0.96	0.07	−0.04
Magnetic susceptibility	0.88	0.06	0.09
Al	0.92	0.13	−0.12
Ba	0.55	−0.03	0.30
Ca	0.92	0.09	0.07
Cr	0.88	0.14	−0.04
Fe	0.96	0.11	−0.12
K	−0.81	0.12	0.46
P	0.79	−0.03	0.25
Rb	−0.26	0.72	0.58
S	0.87	0.07	−0.02
Si	−0.94	−0.12	0.03
Sr	0.81	0.11	−0.13
Ti	0.93	0.11	−0.11
Zr	0.77	−0.12	0.18
% variance	66.21	7.29	6.29
Accumulative %	66.21	73.50	79.79
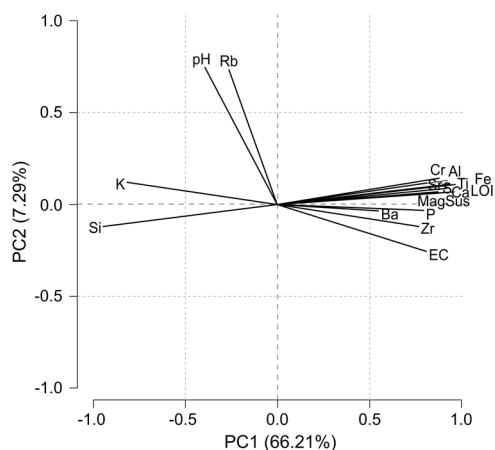
FIGURE 6 Results of the first two principal components for Burghead upper surface.

PC2 accounted for 7.29% of the total variance and demonstrated high loadings (>0.71) for pH and Rb. PC3 accounted for 6.29% of the total variance and presented moderate positive loadings (>0.45) for Rb and K. These elements are known to be strongly correlated in soils, and both PC2 and PC3 are likely to reflect lithogenic signatures (Croffie et al., 2022, p. 819). Across all three PCs, EC showed a negative correlation with pH, indicating that areas with a higher concentration of soluble salts or nutrients were generally more acidic.

4.1.2 | Spatial distributions

Spatial plotting of the individual upper surface variables and interpolation of the PCA results permitted an evaluation of how the PCA variance related to patterning and inputs. PC1 primarily related to an area of anthropogenic contamination at the southern edge of the trench (Figure 7). Here, concentrations of Al, Ca, Sr and Ti were between four and seven times higher than the grid average, with Fe returning concentrations up to eight times higher and S up to 10 times higher (Figure 8). Distribution maps of the elements excluded from statistical analysis showed that this area was also enriched in Cl, Cu, Ni, Pb, V and Zn, and correlated with high concentrations of post-medieval industrial waste (Figure 8—see also File 2). The contaminated area had a high organic content (LOI), suggesting that the elemental enrichment related in part to plant matter and/or human and animal waste, with the area most likely functioning as a 19th-century dump or midden (Bintliff & Degryse, 2022).

Although PC1 was dominated by this area of contamination, it also identified enrichment towards the east of the trench and in the visible extent of surfaces 105 and 106 (Figure 7). Notably, these areas showed little to no enrichment in Cl, Cu, Ni or V, and no coal, clinker or slag was recovered from these areas during microrefuse analysis, suggesting that their geochemical signatures were not associated with the later waste material. Instead, they correlated with elevated charcoal concentrations and likely reflected anthropogenic activity related to the structure and the concentration of postholes in the east (File S2).

The spatial distribution of PC2 corresponded to the area between the two noncontaminated areas identified in PC1 and had very few indications of habitation, returning some of the lowest values for magnetic susceptibility, organic matter content and plant macronutrients (Ca, P and S), alongside a comparative lack of charcoal (Figures 7 and 8). PC3 further differentiated surface 105 and the eastern posthole area identified in PC1.

4.2 | Burghead lower surface (containing 106)

4.2.1 | PCA results

Four principal components were chosen for analysis according to the Kaiser criterion (Kaiser, 1960, 1970) and accounted for 72.87% of the total variance of the geochemical record (Table 2).

PC1 accounted for 46.78% of the total variance and appeared to reflect areas with a higher organic content and a lower mineral component, demonstrating high positive loadings (>0.70; Table 2) for nine of the variables and negative loadings (>−0.55) for Si and pH (Figure 9). The positively correlated elements included common
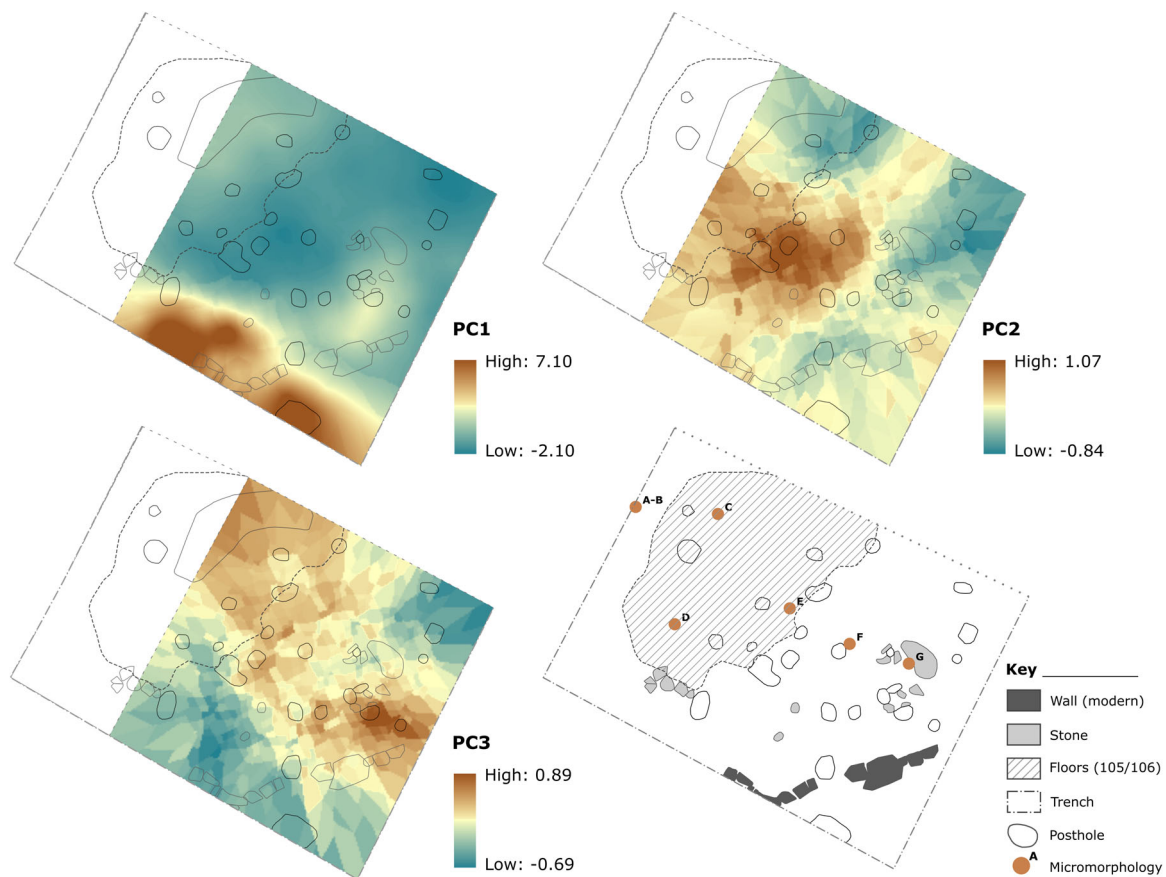
FIGURE 7 Interpolation of Burghead upper surface principal component analysis results—positive loadings brown, negative loadings blue—with a feature map (bottom right) to aid interpretation.

indicators of human habitation such as Ca, P and elevated magnetic susceptibility—the latter indicating the presence of particles that had been magnetically enhanced by heating (Bintliff & Degryse, 2022; Milek & Roberts, 2013, p. 1853). Strong positive loadings (>0.70) for EC, LOI, plant macronutrients (Ca, P and S) and groundwater trace elements (Sr) reflected an increased organic component that could result from the deposition of plant or wood materials or their ashes (Bintliff & Degryse, 2022; Davidson et al., 2007; Entwistle et al., 2007; Jones et al., 2010; Wilson et al., 2005). This was corroborated by a strong negative loading (>−0.71) for Si (the primary mineral component of sand) and was also reflected in the micromorphology (sample BHF16-C), which contained the highest values of charred organic matter (2%–5%) for 106 in this area of the site (Table 3). However, the accompanying positive correlation for Ti complicates the interpretation. Ti is a natural weathering product of silicate rock and is generally indicative of a high mineral content rather than anthropogenic or organic inputs (Knudson et al., 2004, p. 451).

PC2 demonstrated moderate to high loadings (0.40–0.91) for lithogenic elements (Al, Ba, K, Rb and Si) and most likely captured the natural variability of elements in Burghead's quartz and feldspar sands (Benton et al., 2002, pp. 31–41). PC4 also demonstrated positive loadings for elements associated with the

weathering of silicate rock (Si, Ti and Zr) that appeared to reflect the local sandstone geology (Garcia et al., 1994). PC3 demonstrated the inverse relationship between pH and EC, in which areas of lower pH typically had a higher nutrient/soluble salt concentration.

4.2.2 | Spatial distributions

The positively correlated elements of PC1 appeared to capture localised anthropogenic enrichment associated with the visible extent of occupation deposit 106 (Figure 10). The suite of variables included elevated magnetic susceptibility, loss-on-ignition, EC and plant macronutrients (P, Ca and S), which suggests the presence of soil-rich organic deposits, such as peat or turf, that decomposed/burnt in situ, or that was spread or trampled across the interior of the structure (Nesbitt et al., 2013, p. 14). However, micromorphological evidence for burnt peat or turf was lacking, as only trace amounts of rubified fine material were present in thin-section BHF16-C (see Section 4.3.1). Distribution maps of the elements excluded from statistical analysis showed that this area was also enriched in Zn (another

FIGURE 8 Selected spatial results from Burghead deposit 105 single variable analysis; distributions of industrial waste material, percent organic matter (loss-on-ignition at 550°C), magnetic susceptibility, and percent elements Ca (calcium), Cu (copper), Fe (iron), P (phosphorus) and S (sulphur)—results sorted according to natural breaks (Jenks).

organic matter indicator) and moderately correlated with concentrations of charcoal (Figure 11).

An additional area of anthropogenic enrichment was identified by PC1 in the southwest corner of the trench and correlated with the highest concentration of charcoal recovered from the lower surface. Its location may indicate an extension of surface 106 or represent the remains of a burnt and degraded turf wall (as suggested by the field evidence from the 2017 trench—Figure 3). The moderate negative loading of pH showed that these areas were among the most acidic on the site.

A moderately positive loading of PC1 was also present in the south-central part of the occupation surface, which showed particularly high EC values (Figure 11). Ten of the 13 elements subjected to statistical analysis showed positive correlations with EC that were statistically significant at the 0.01 level (File S3). However, only the element distribution maps of S and Fe (and to a lesser extent Ca and P), and the distribution of LOI (organic matter) corresponded to the spatial pattern of EC elevation observed in the south of the trench (Figure 11), suggesting that a deposit of organic matter was responsible for elevated PC1 in this area.

TABLE 2 Results of the first four principal components for Burghead lower surface, showing loadings and % of the variance explained.

Components	PC1	PC2	PC3	PC4
pH	−0.57	0.02	0.70	0.13
Electrical conductivity	0.71	−0.11	−0.61	−0.01
Loss-on-ignition	0.94	−0.15	0.03	0.05
Magnetic susceptibility	0.82	−0.08	0.00	0.12
Al	0.44	0.74	−0.10	0.10
Ba	0.22	0.50	0.17	−0.29
Ca	0.87	−0.09	0.33	−0.03
Cr	0.51	0.12	−0.16	−0.48
Fe	0.89	−0.09	0.03	0.06
K	0.03	0.91	−0.09	0.09
P	0.78	0.08	0.20	−0.08
Rb	0.40	0.48	0.14	0.13
S	0.89	−0.10	−0.07	−0.01
Si	−0.71	0.40	−0.18	0.30
Sr	0.76	0.06	0.37	−0.17
Ti	0.85	0.07	0.03	0.30
Zr	0.41	−0.18	0.00	0.66
% variance	46.78	12.48	7.57	6.04
Accumulative %	46.78	59.26	66.83	72.87
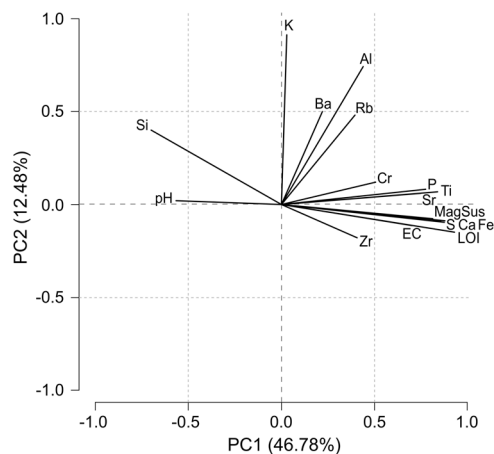
FIGURE 9 Results of the first two principal components for Burghead lower surface.

4.3 | Burghead micromorphology

4.3.1 | Surfaces 105 and 106

Micromorphology samples BHF16-C and BHF16-D were taken from a baulk across the structure to investigate the preservation and composition of the black sandy layers believed to be floors. Their location lay just outside of the sampling grid for the upper occupation deposit (105) but within the lower occupation deposit (106), where they related to the area of PC1 that demonstrated the highest loadings and values for magnetic susceptibility, organic matter content, EC and plant macronutrients (P, Ca and S) (Figures 10 and 11). In these thin sections, the upper (105) and lower occupation deposits (106) were very similar. They were composed predominantly of quartz and feldspar sands, and the black colour observed in the field had been imparted by low frequencies (2%–10%) of charred and uncharred organic matter, most of which was adhering to the sand grains in the form of irregular coatings or existed as dark brown to black intergrain microaggregates that included soil fauna excrements (Table 3; Figure 13a; detailed descriptions, section drawings and interpretations in File S1). The deposits had been extensively bioturbated and the organic coatings around the sand grains appear to have been formed through a combination of soil fauna activity and localised redistribution by rainwater percolating through the deposits. Organic matter and microaggregate concentrations decreased down the profile, with layer 106 slightly less organic-rich than 105; trace amounts of rubified fine material and iron nodules characteristic of peat and turf ash were also present in 106 in BHF16-C. These layers were therefore confirmed to be occupation deposits on the basis of both the geochemical and micromorphological evidence but had no surviving evidence of trampling, compaction or other characteristics normally used to identify floors, due to extensive post-depositional alteration by bioturbation.

4.3.2 | Surfaces 105 and 106 on the western trench edge

The two thin sections taken from the western trench edge, samples BHF16-A and BHF16-B, also captured the upper and lower surfaces identified in BHF16-C and BHF16-D, and were located in a zone where all PCs (particularly PC2 and PC3) showed high loadings (Figures 7 and 10). While a high degree of eluviation and bioturbation was still evidenced by earthworm channels, organic coatings and intergrain microaggregates, the upper surface (105) in this area was found to have a markedly different composition and preservation, containing several micro-artefacts not identified elsewhere on the site (Figure 12). Here, 105 contained the highest charred organic matter content of any sample (5%–10%), with larger and more frequent fragments of charcoal that included pine (*Pinus* sp.), charred monocot stems and a charred cereal grain. The upper surface also contained wood ash in the form of aggregates of silt-sized calcium carbonate, and several aggregates of grey clay that had a platy microstructure, parallel and subparallel planar voids (10% porosity) and a unistriated b-fabric. In one instance, the clay was found coating a large charcoal fragment (4 × 21 mm) that may be evidence of charred wattle-and-daub, with the unistriated b-fabric and planar voids resulting from a 'smearing' action

TABLE 3 Summary of descriptive sediment attributes, inclusions and post-depositional alterations at Burghead.

	Structure			Void types[a]			Fine material		
Slide/unit	Textural class	Microstructure	Course:fine (100 μm) ratio	Channels	Simple packing voids	Complex packing voids	Nature of fine material (PPL)	Colour of fine material (OIL)	Birefringence fabric (XPL)
A105	Medium-course sand	Intergrain microaggregate	92:8	▪▪▪▪▪		▪▪▪▪▪▪▪▪	Very dark brown; black; dotted	Very dark brown; black	Undifferentiated
A106	Medium-course sand	Intergrain microaggregate	96:4	▪▪▪▪▪	▪	▪▪▪▪▪▪▪▪	Brown; dark brown; dotted	Dark brown	Undifferentiated
B106	Medium-course sand	Intergrain microaggregate	98:2	▪▪▪▪▪	▪▪	▪▪▪▪▪▪▪	Very dark brown; black; dotted	Very dark brown; black	Undifferentiated
C105	Medium-course sand	Intergrain microaggregate; localised pellicular	93:7	▪▪▪	▪	▪▪▪▪▪▪▪▪	Very dark brown; black; dotted	Very dark brown; black	Undifferentiated
C106	Medium-course sand	Intergrain microaggregate; localised pellicular	97:3	▪▪▪	▪▪▪	▪▪▪▪▪▪▪	Very dark brown; black; dotted	Very dark brown; black	Undifferentiated
D105	Medium-course sand	Intergrain microaggregate; localised pellicular	93:7	▪▪▪▪	▪▪	▪▪▪▪▪▪▪▪	Very dark brown; black; dotted	Very dark brown; black	Undifferentiated
D106	Medium-course sand	Intergrain microaggregate; localised pellicular	97:3	▪▪▪▪	▪▪▪	▪▪▪▪▪▪▪	Very dark brown; black; dotted	Very dark brown; black	Undifferentiated
E106[b]	Medium-course sand	Intergrain microaggregate; localised single-grain	97:3	▪▪▪	▪▪▪▪▪▪▪	▪▪▪▪▪	Dark brown; dotted	Dark brown	Undifferentiated
F106[b]	Medium-course sand	Single-grain; localised intergrain microaggregate	99:1	▪▪	▪▪▪▪▪▪▪	▪▪▪▪▪▪	Dark brown; dotted	Dark brown	Undifferentiated
G106[b]	Medium-course sand	Intergrain microaggregate	96:4	▪▪▪▪	▪▪▪▪	▪▪▪▪▪▪▪▪	Dark brown; dotted	Dark brown	Undifferentiated

	Organic matter			Inclusions			Pedofeatures	
Slide/unit	Charred	Uncharred	Wood ash	Aggregates (clay)	Aggregates (other)	Rubified fine material	Fe/Mn	Excremental
A105	▪▪▪▪	▪▪	▪	▪▪		▪	+	▪▪
A106	+	▪▪			▪		+	▪▪
B106	▪	▪			▪▪	+		▪
C105	▪	▪▪						▪▪
C106	▪▪	▪▪				+	+	▪
D105	▪	▪▪▪						▪▪▪

(Continues)

TABLE 3 (Continued)

Slide/unit	Organic matter		Inclusions		Aggregates (clay)	Aggregates (other)	Rubified fine material	Pedofeatures	
	Charred	Uncharred	Wood ash					Fe/Mn	Excremental
D106	▪	▪▪							▪▪
E106[b]	+	▪▪							▪▪
F106[b]	+	▪							▪
G106[b]	+	▪▪							▪▪

Abbreviations: +, present in trace amounts; ▪, <2%; ▪▪, 2%–5%; ▪▪▪, 5%–10%; ▪▪▪▪, 10%–20%; ▪▪▪▪▪, 20%–30%; ▪▪▪▪▪▪, 30%–40%; ▪▪▪▪▪▪▪, 40%–50%; ▪▪▪▪▪▪▪▪, 50%–60%; ▪▪▪▪▪▪▪▪▪, 60%–70%; ▪▪▪▪▪▪▪▪▪▪, >70%; OIL, oblique incident light; PPL, plane-polarised light; XPL, cross-polarised light.

[a]Void frequency refers to % total void space (following Bullock et al., 1985; Stoops, 2021, p. 73).

[b]Labelled as (106) during excavation but do not represent an extension of the lower floor (106).

(Friesem et al., 2017, pp. 104–106; Milek & French, 2007, p. 338) (Figure 13c,d). Anthropogenic inclusions were unique to this thin section and layer and were unusually well preserved, given the extensive eluviation and bioturbation throughout. This may reflect the more favourable preservation identified in the 2017 trench or represent increased anthropogenic activity towards the end of the structure associated with the hearth. It may also be evidence of a contemporary wattle partition or wall-panelling that burnt in situ.

The parts of context 106 captured in samples A and B on the western trench edge were similar to those captured in the baulk, in that they contained no anthropogenic inclusions other than trace charcoal and decreased in organic matter and microaggregate concentrations down the profile. One notable difference was the inclusion of two different fabric types: Fabric 1 comprised localised aggregates of yellowish-brown clayey-silt with a massive microstructure and speckled b-fabric, whilst Fabric 2 existed as discrete aggregates and 1 mm thick intercalations (sensu Stoops, 2021, p. 174) of loamy sand with very angular quartz grains and undifferentiated b-fabric (Figure 13e). As with the inclusions in 105, these were only captured in the samples taken from the western trench edge. They are likely to have resulted from anthropogenic activity such as digging and trampling; however, the precise origin of this material is unknown as a source did not become apparent during the excavation or in thin section.

4.3.3 | Eastern area

Thin sections BHF16-E, BHF16-F and BHF16-G were taken from the area east of the visible layer 106 to investigate whether the lower surface continued, had been truncated by later activity, or represented different depositional or post-depositional processes. All three were found to have been subjected to the same post-depositional processes as 106, showing a highly eluviated and bioturbated surface containing intergrain microaggregates with no surviving microstructure of a relict floor. However, the samples were differentiated from the known extent of the surface based on lower quantities of charred and amorphous organic matter. All three thin sections contained only trace amounts of charred material, and whilst the quantities of amorphous organic matter in BHF16-E and BHF16-G were comparable with the values recovered from the visible extent of 106 (2%–5%), BHF16-F had significantly fewer microaggregates and less amorphous organic matter (<1%). Due to this difference, the fine material from the eastern area appeared lighter in colour under PPL and OIL to that observed in samples BHF16-B, BHF16-C and BHF16-D (dark brown vs. very dark brown/black). This correlated strongly with the visibility observed in the field. Given these differences in field, geochemical and micro-morphological evidence, there is little evidence to suggest that these deposits represent a continuation or survival of the lower floor 106 in the eastern area of the trench.
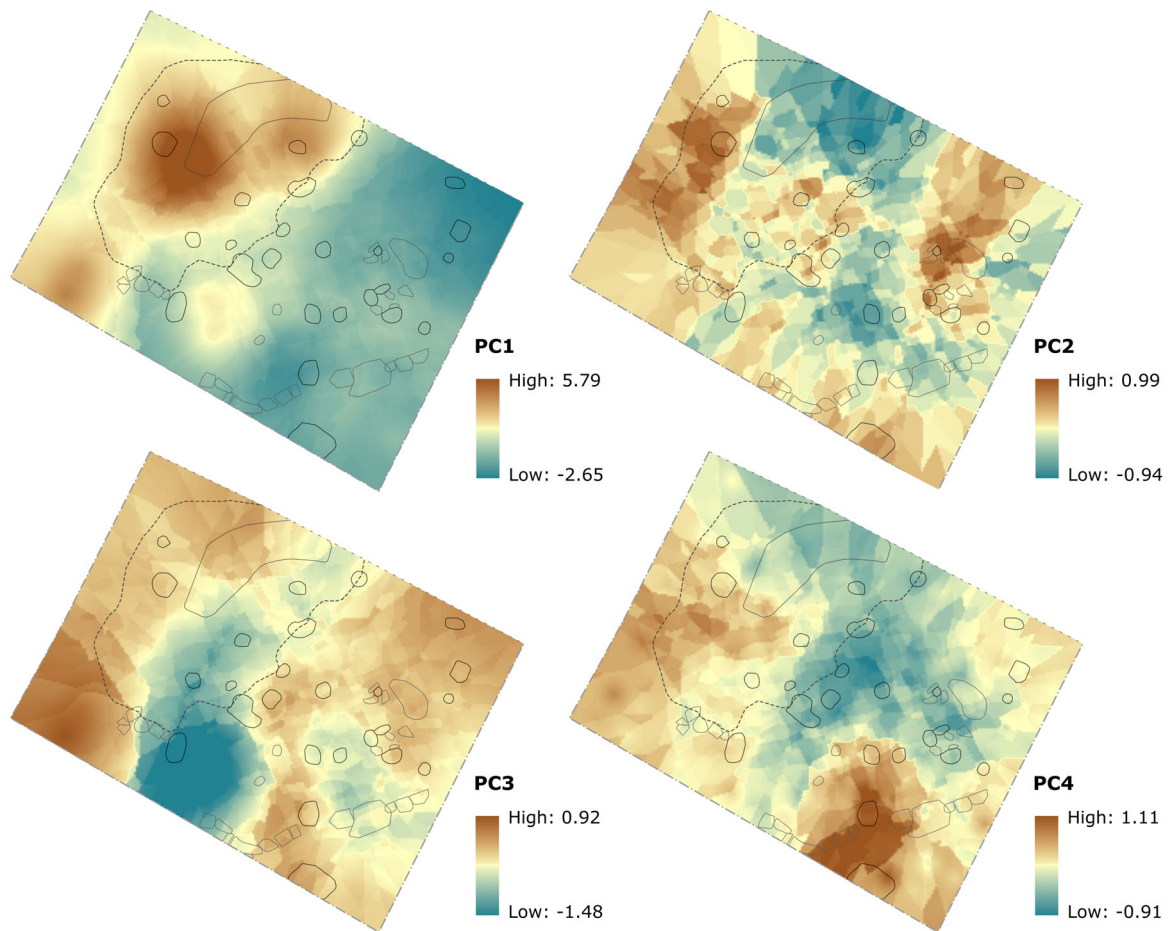
FIGURE 10 Interpolation of Burghead lower surface principal component analysis (PCA) results—positive loadings brown, negative loadings blue. For interpretation of the references to colour in this figure, the reader is referred to the web version of this article.

4.4 | Dunnicaer

### 4.4.1 | Spatial distributions and correlations

Despite the small excavation area at Dunnicaer, the distribution maps and statistical correlations indicated variability and clustered distribution patterns within Dunnicaer's lower terrace. There was a clear positive correlation (r_s up to 0.87) between Ba, Ca, Mn, P, Sr and Zn that related to the area in and immediately north of the hearth (Tables 4 and 5; Figure 14). Elevation in these particular elements has been demonstrated in midden and hearth areas of settlements elsewhere in Scotland, comprising trace elements and plant macronutrients most often linked to the decomposition or burning of plant matter and excreta (Bintliff & Degryse, 2022; Davidson et al., 2007; Entwistle et al., 1998; Wilson et al., 2005, 2008). Mn and Zn have more specifically been linked to animal dung and manure, perhaps indicating their use as a fuel source (Bintliff & Degryse, 2022; Ottaway & Matthews, 1988, p. 4). Elevations in Ca and Sr have been argued to derive from the specific inclusion of bone waste and broadly correlated with the distribution of burnt bone observed at Dunnicaer (with both returning the highest values in the northeast trench corner) (Knudson et al., 2004, p. 449; Nielsen & Kristiansen, 2014).

Whilst the overall pH range was narrow (4.1–5.5), samples collected from the hearth and surrounding deposits were the least acidic (pH 5.1–5.5) and corresponded to elevated EC values, indicating very high nutrient or soluble salt levels associated with the deposition of ash. Though the suite of elements mentioned above were elevated in this area, the correlation coefficient (r_s) only showed a strong positive correlation for EC with Cu and Zn, which was statistically significant at the 0.01 level (Table 5). Charcoal and bone are believed to play a role in both the loading and post-depositional retention of Ca, Sr, P, Zn and Cu, suggesting that the soil element concentration patterns within this area are likely related to these hearth residues (Davidson et al., 2007; Wilson et al., 2008).

Elevated organic matter content was observed in the southwest corner of the trench, correlating positively (r_s up to 0.91, $p = 0.01$) with plant macronutrients P and S, and to some extent magnetic susceptibility and Mn, and negatively ($r_s > -0.72$, $p = 0.01$) with lithogenic elements K, Si and Ti (Table 5; Figure 11). It is notable that the highest values of magnetic susceptibility were not recorded in/around the hearth itself but were more closely associated with the southern edge of the trench and the charcoal patch 1007, which was interpreted in the field as hearth rake-out. The magnetic enhancement of this area indicates the presence of soil particles, pebbles
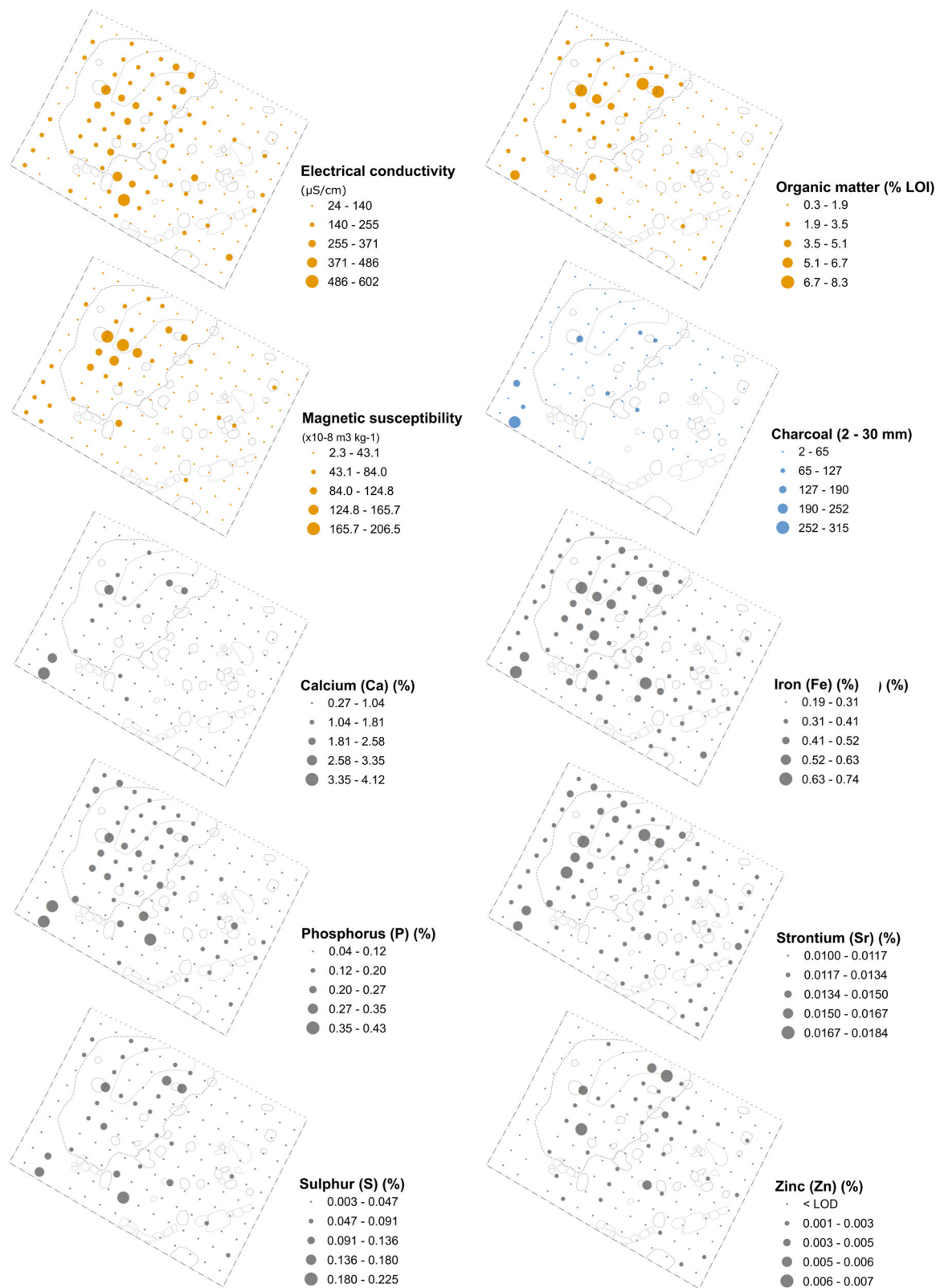
FIGURE 11   Selected spatial results from Burghead lower surface single variable analysis; distributions of electrical conductivity (EC), percent organic matter (loss-on-ignition at 550°C), magnetic susceptibility, charcoal and percent elements Ca (calcium), Fe (iron), P (phosphorus), Sr (strontium), S (sulphur) and Zn (zinc)—results sorted according to equal intervals.
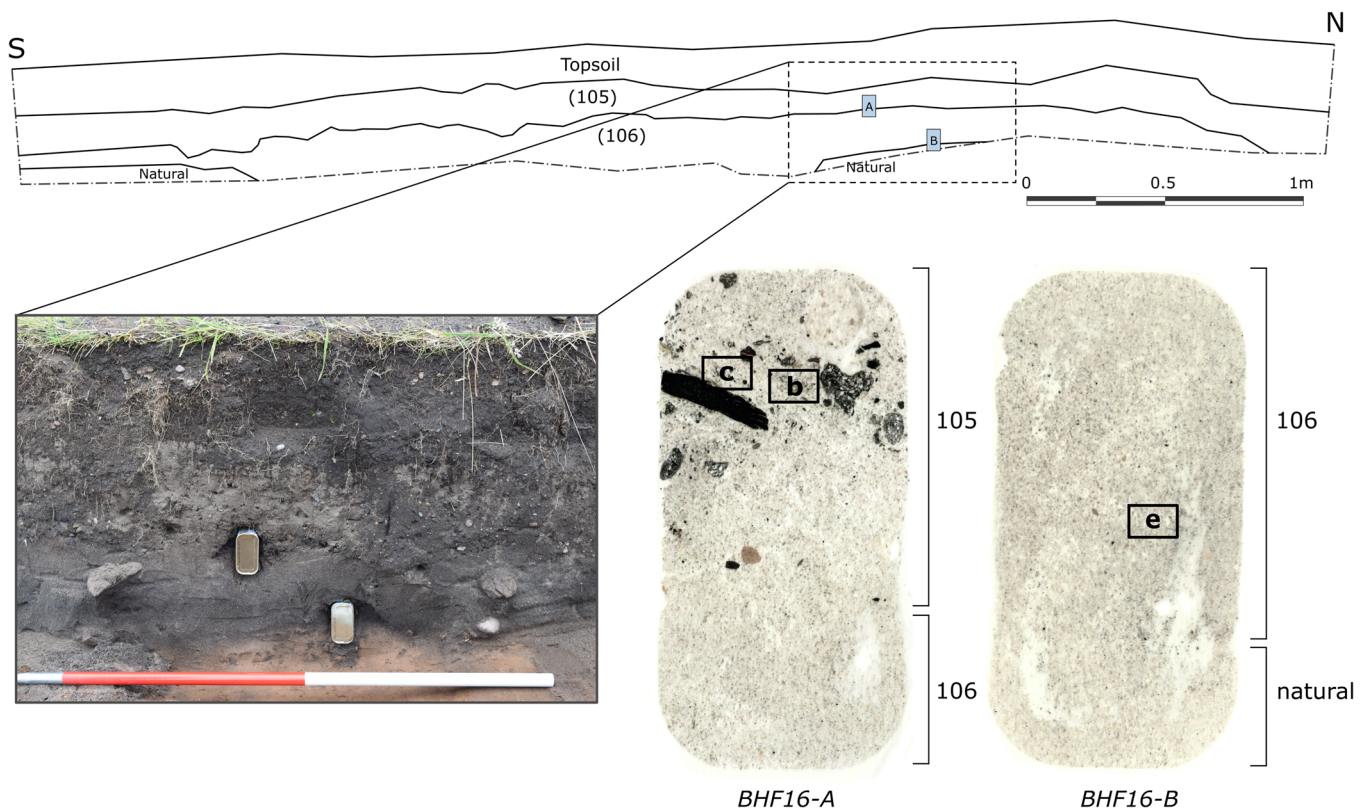
FIGURE 12 Scans of Burghead thin sections BHF16-A (centre) and BHF16-B (right) with photograph of soil blocks in section (left) and section drawing (top) showing sampled stratigraphy and location of photomicrographs in Figure 13.

and/or iron nodules that were affected by heating (Milek & Roberts, 2013, p. 1853). This suggests that heated soil material from the base of the hearth may have mixed with ash residues, and perhaps also signals the use of soil-rich fuel sources such as peat or turf, though micromorphological evidence for this was limited (see Section 4.5) (Milek & Roberts, 2013, p. 1853; Nesbitt et al., 2013, p. 14).

There was a comparative depletion in habitation indicators in the area east of the hearth that correlated with elevations in the lithogenic elements Al, K, Si, Ti and Zr (Figure 14; File S4). This area lay between areas of raised bedrock (Figure 5) and marked the natural passage from the upper terrace to the lower terrace during excavation, perhaps having performed a similar function in the past. It also related to the hard-packed deposit of what appeared to be redeposited natural sediment lying directly above the bedrock on the eastern edge of the trench. Should this have indeed functioned as a levelling surface, it may have become incorporated into the floor layers through repeated trampling.

4.5 | Dunnicaer micromorphology

The three thin sections taken from the eastern side of the lower terrace sondage contained layers related to occupation surfaces and the modification of the lower terrace. Four separate lenses were

identified in floor 1009 (subcontexts 1009.1–1009.4—Figure 15), all of which comprised sandy silt loams with a porphyric c/f-related distribution, subangular blocky microstructure, 5%–20% amorphous decomposed organic matter and extensive staining by organic acid pigmentation. Phytoliths were not readily identifiable in any of the layers and may have been masked by this staining.

Despite the lenses having been reworked by soil fauna, the horizontal orientation of charcoal and minerals was observable to varying degrees, with subcontext 1009.2 also containing a significant percentage of horizontal planar voids that result from vertical compaction (10%–20%) (Table 6; Figure 16). These are key indicators of trampling on occupation surfaces (see Rentzel et al., 2017), supporting the field interpretation of floor layers within the structure's interior. Lenses 1009.3 and 1009.4 showed an intra-aggregate crumb structure that is likely related to post-depositional reworking by soil fauna but may also reflect the nature of the material used to form the surface (e.g., turf or redeposited topsoil). 1009.4 also contained multiple sublinear areas (max. 27 × 3 mm) of darker, more organic material with lower porosity, which may be evidence of compaction and/or further evidence for the use of organic material such as turf. Given that preceding context 1011 related to the lower hearth, this likely represents a rebuilding episode contemporary with the construction of the new hearth.

The two thinnest lenses (1009.1 and 1009.3) were 15 mm thick and were significantly richer in charred material (10%–20%). They
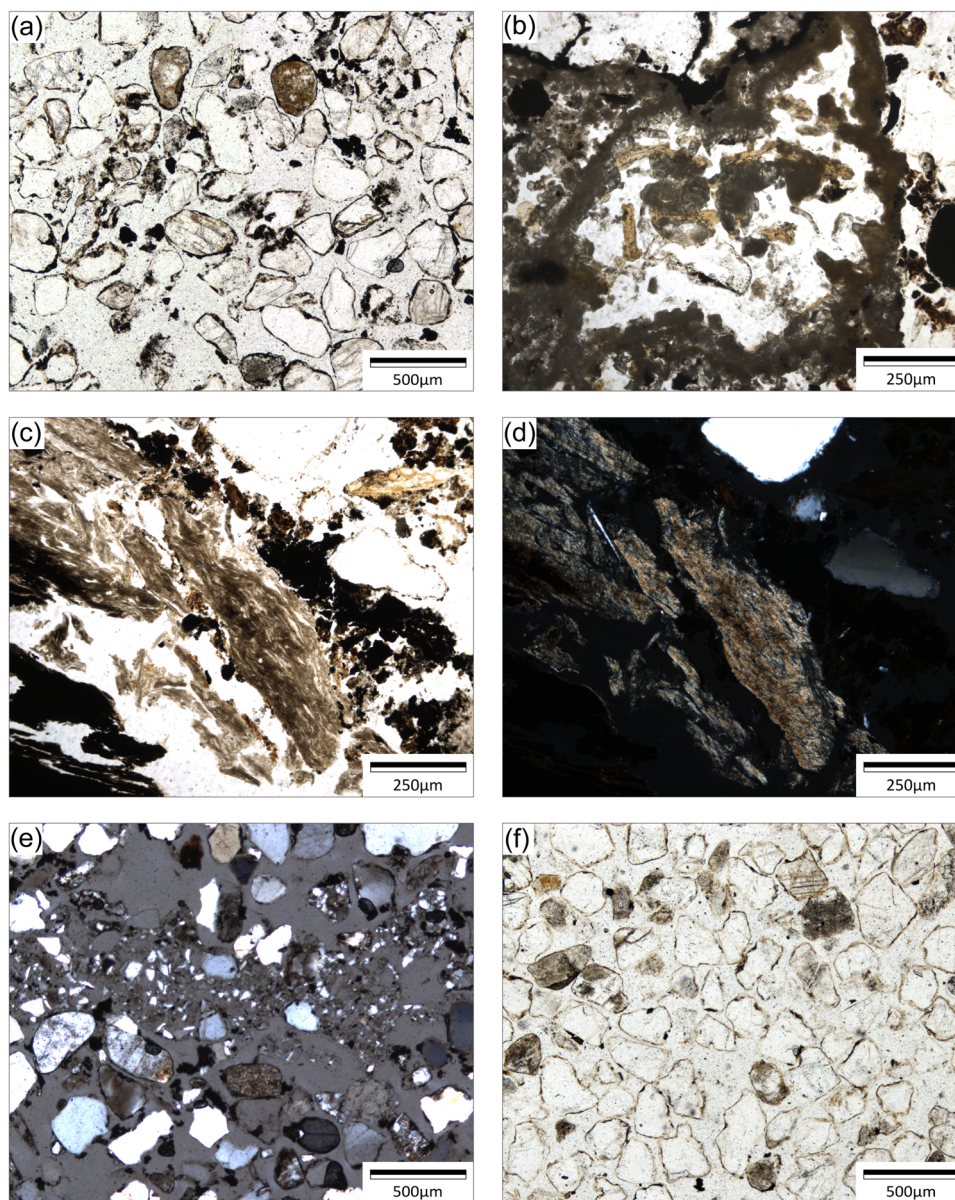
FIGURE 13 Photomicrographs of Burghead thin sections, (a) BHF16-C, context 106, showing the intergrain microaggregate structure of the relict floor (plane-polarised light [PPL]); (b) BHF16-A, context 105, showing wood ash in the form of aggregates of micrite and poorly preserved bone fragments (PPL); (c) BHF16-A, context 105, showing clay daub fragment with a platy microstructure, parallel and subparallel planar voids (PPL); (d) as described previously, showing unistriated b-fabric (XPL); (e) BHF16-B, context 106, showing Fabric 2 intercalation (partial XPL); and (f) BHF16-F, single-grain microstructure with localised intergrain microaggregate demonstrating lack of amorphous organic material in comparison with (a) (PPL).

appeared to alternate with layers up to 75 mm thick, perhaps indicating a maintenance practice that involved the treatment or filling of well-worn floor deposits with hearth refuse. Although the highest values of magnetic susceptibility were associated with the southern edge of the trench and the charcoal patch 1007, which was interpreted in the field as hearth rake-out, direct evidence of wood ash was not identified in thin section, likely due to dissolution in free-draining acidic conditions. Similarly, although burnt bone was recovered during microrefuse analysis, none of the layers in context 1009 contained anthropogenic inclusions other than varying quantities of diffuse

porous charcoal (1%–10%) (*Corylus* sp. and *Betula* or *Salix/Populus* sp.). Lens 1009.2 did contain a cluster of strongly decomposed circular organic material (Figure 16b) that appeared similar in size and shape to the excremental pedofeatures found throughout the lens (Figure 16d), although was differentiated by a greater and more consistent opaqueness under PPL and OIL. However, the extent of decomposition meant that it was not possible to explore the nature or source of this material further. Quantities of rubified iron nodules characteristic of peat and turf ash were only present in trace or very low amounts (<2%).

TABLE 4 Most highly correlated variables ($r_s > 0.70$).

Variables		Correlation coefficient
Loss-on-ignition (LOI)	S	0.91
Ca	Sr	0.87
Ba	Mn	0.86
Ba	Zn	0.81
Mn	Zn	0.79
LOI	K	−0.79
K	Ti	0.78
LOI	Si	−0.77
Si	Ti	0.77
LOI	Ti	−0.73
Al	K	0.73
K	S	−0.72
S	Si	−0.71
K	Si	0.71

Sample DUNC16-C captured the floor (1011) associated with the lower hearth. A large earthworm channel and Fe plant pseudomorph restricted the space available for analysis (Figure 15); however, the shallowness of this deposit in comparison to the cumulative lenses of 1009 was notable—particularly given the evidence for the lower hearth's extensive use (Noble et al., 2020, p. 284). This is perhaps evidence of different maintenance practices relating to the lower hearth, or the removal of cumulative layers before the building of the new hearth. As with 1009, no anthropogenic inclusions other than charcoal (*Betula* or *Salix/Populus* sp. and *Corylus* sp.) and plant matter were identified within the layer. DUNC16-C also identified the earliest archaeological layer (1013) lying directly above the bedrock, which comprised a sandy silt loam and angular gravel-sized rock fragments (up to 1.5 cm in size). This was likely deposited during the primary construction of the structure to level the lower terrace hollow and create a suitable occupation surface or foundation for a structure.

5 | DISCUSSION

5.1 | Burghead

The most obvious anthropogenic signature at Burghead was an area of industrial contamination in the upper surface (Figure 17). The geochemical data and interpolated PCA confined the extent of its impact to the southern end of the trench, indicating that the surrounding material was more 'authentically' archaeological in nature. They also permitted a characterisation of post-medieval industrial waste containing coal, clinker, cinder and slag, which was differentiated from archaeological material by an up to 10-fold increase in element concentration and, more specifically, the presence of Cl, Cu, Ni and V.

The visible extents of surfaces 105 and 106, which were identified during excavation, were reflected in both the micro-morphological and geochemical data sets, most convincingly in the spatial and statistical analyses of the lower surface, which was characterised by enhanced soluble salt concentrations, magnetic mineral signatures and chemical elevations associated with organic matter. This appeared to represent the remains of a decomposed burnt turf wall and/or an organic floor that may have had soil-rich ash spread across the structure interior. The practice of spreading ash is known from 10th-century Iceland (Milek & Roberts, 2013), post-medieval Scottish crofts (Nesbitt et al., 2013; Smith, 1996) and 19th/20th-century ethnography (Fenton, 1978, p. 195; Milek, 2012), where the floors of turf houses were treated to absorb moisture and odours. Recent evidence from a comparative geoarchaeological study at Lair in Glen Shee (central Scotland) suggests that this was also practiced on 7th- to 9th-century Pictish farmsteads (Reid et al., 2023). Though geochemical signatures in the upper surface were dominated by contamination, a pattern of element enrichment also seemed to correlate with the eastern end of 105 and 106.

Micromorphological evidence of a clay-coated charcoal fragment in the upper surface offers limited but tangible evidence that wattle-and-daub formed part of the construction of Building 2. The location might suggest a separation of the hearth/living area from another 'room' or storage area in the east (represented by surfaces 105/106) or may be evidence of panelling on the interior walls. The former hypothesis is perhaps more likely, given that the PCA results of the lower surface, particularly PC1, indicated a western 'edge' to the activity area (Figures 10, 17 and 18). An internal panel coated with clay was also hypothesised at the Pictish farmstead at Lair, where a fragment of daub was found together with clear evidence of animal housing and an internal division (Reid et al., 2023; Strachan et al., 2019, p. 103). The presence of wood ash alongside the charred clay/charcoal fragments could indicate that the upper surface captured in the western end of the trench relates to the burning event observed in the north of the structure, rather than a continuation of the upper floor layer (105) as originally thought. Should this be the case, the visible extent of 105 in the field may not be a superseding floor at all, but rather turf slump and/or roof collapse associated with the burning event and subsequent degradation. It may alternatively represent a later dumping episode of unknown date.

Neither the geochemical data nor micromorphological evidence indicated that the structure extended eastwards beyond the visible limit of 105/106, which appeared to end at a concentration of postholes in the centre of the trench (Figure 18). The integrated geoarchaeological evidence therefore contributed

TABLE 5 Dunnicaer correlation analysis based on Spearman's rho (r_s) for geochemical and multi-element values.

	pH	EC	LOI	Mag Sus	Al	Ba	Ca	Cl	Cr	Cu	Fe	K	Mg	Mn	P	Pb	Rb	S	Si	Sr	Ti	V	Zn	Zr
pH	1.00																							
Electrical conductivity (EC)	0.12	1.00																						
Loss-on-ignition (LOI)	-0.66**	-0.10	1.00																					
Mag Sus	-0.20	0.33	0.34	1.00																				
Al	0.31	-0.41*	-0.50*	0.03	1.00																			
Ba	0.05	0.48**	0.03	0.54**	-0.12	1.00																		
Ca	0.52**	0.29	-0.33	0.22	0.19	0.65**	1.00																	
Cl	-0.63**	0.09	0.54**	0.46*	-0.21	0.00	-0.31	1.00																
Cr	0.04	0.07	0.05	0.13	0.18	0.23	0.09	-0.18	1.00															
Cu	-0.12	0.64**	0.30	0.56**	-0.34	0.57**	0.27	0.20	0.31	1.00														
Fe	-0.15	-0.19	0.40	0.57**	0.28	0.17	0.08	0.47*	0.29	0.18	1.00													
K	0.44*	-0.19	-0.79**	-0.37	0.73**	-0.17	0.29	-0.41*	0.13	-0.38	-0.10	1.00												
Mg	0.45*	0.00	-0.51*	-0.14	0.41*	-0.12	0.08	-0.29	0.07	0.11	-0.04	0.54**	1.00											
Mn	0.08	0.44*	0.14	0.70**	-0.05	0.86**	0.62**	0.02	0.38	0.62**	0.31	-0.24	-0.21	1.00										
P	-0.22	0.13	0.54**	0.57**	-0.25	0.66**	0.35	0.26	0.29	0.50*	0.56**	-0.51*	-0.41*	0.69**	1.00									
Pb	0.22	0.51**	-0.33	0.14	0.22	0.30	0.39	-0.11	0.24	0.45*	-0.05	0.30	0.44**	0.15	-0.04	1.00								
Rb	-0.37	-0.40	0.45*	-0.11	0.00	-0.35	-0.45*	0.22	0.14	-0.21	0.25	-0.08	-0.18	-0.26	0.13	-0.42*	1.00							
S	-0.56**	-0.18	0.91**	0.35	-0.32	0.05	-0.25	0.52**	0.09	0.26	0.54**	-0.72**	-0.53**	0.19	0.66**	-0.34	0.47*	1.00						
Si	0.42*	-0.29	-0.77**	-0.53**	0.58**	-0.26	0.05	-0.59**	-0.12	-0.57**	-0.42*	0.71**	0.47*	-0.35	-0.65**	0.09	-0.17	-0.71**	1.00					
Sr	0.55**	0.20	-0.43*	0.17	0.36	0.45*	0.87**	-0.37	0.03	0.24	0.10	0.37	0.22	0.48*	0.22	0.39	-0.54**	-0.28	0.10	1.00				
Ti	0.39	-0.10	-0.73**	-0.55**	0.51**	-0.38	0.02	-0.26	-0.13	-0.47*	-0.28	0.78**	0.51**	-0.55**	-0.69**	0.35	-0.15	-0.67**	0.77**	0.05	1.00			
V	-0.05	-0.12	-0.05	0.47*	0.54**	-0.03	-0.05	0.33	0.21	0.01	0.66**	0.26	0.02	0.10	0.12	0.09	0.14	0.08	-0.15	0.11	-0.02	1.00		
Zn	0.16	0.60**	-0.28	0.56**	0.04	0.81**	0.70**	0.03	0.22	0.57**	0.10	0.13	0.04	0.79**	0.35	0.39	-0.48*	-0.25	-0.13	0.57**	-0.13	0.13	1.00	
Zr	-0.17	0.01	-0.08	-0.06	-0.08	0.11	0.00	0.07	0.04	0.04	-0.28	-0.04	-0.20	0.13	-0.05	-0.25	-0.10	-0.06	0.09	-0.07	-0.13	-0.05	0.18	1.00

*Correlation is significant at the 0.05 level (two-tailed).

**Correlation is significant at the 0.01 level (two-tailed).
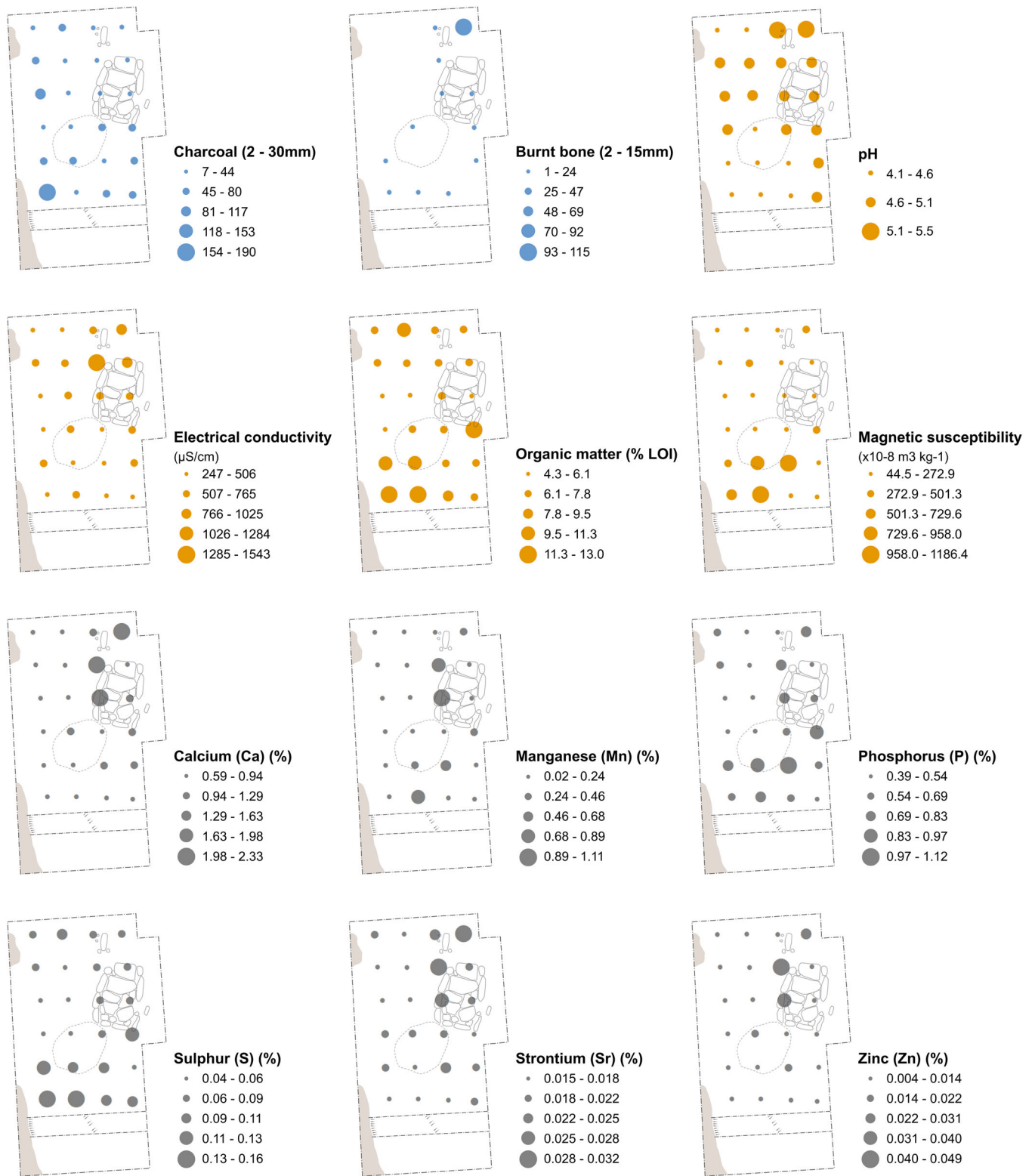
FIGURE 14 Selected results from Dunnicaer spatial analysis—distributions of charcoal, burnt bone, pH, electrical conductivity (EC), percent organic matter (loss-on-ignition at 550°C), magnetic susceptibility and percent elements Ca (calcium), Mn (manganese), P (phosphorus), S (sulphur), Sr (strontium) and Zn (zinc)—results sorted according to equal intervals.
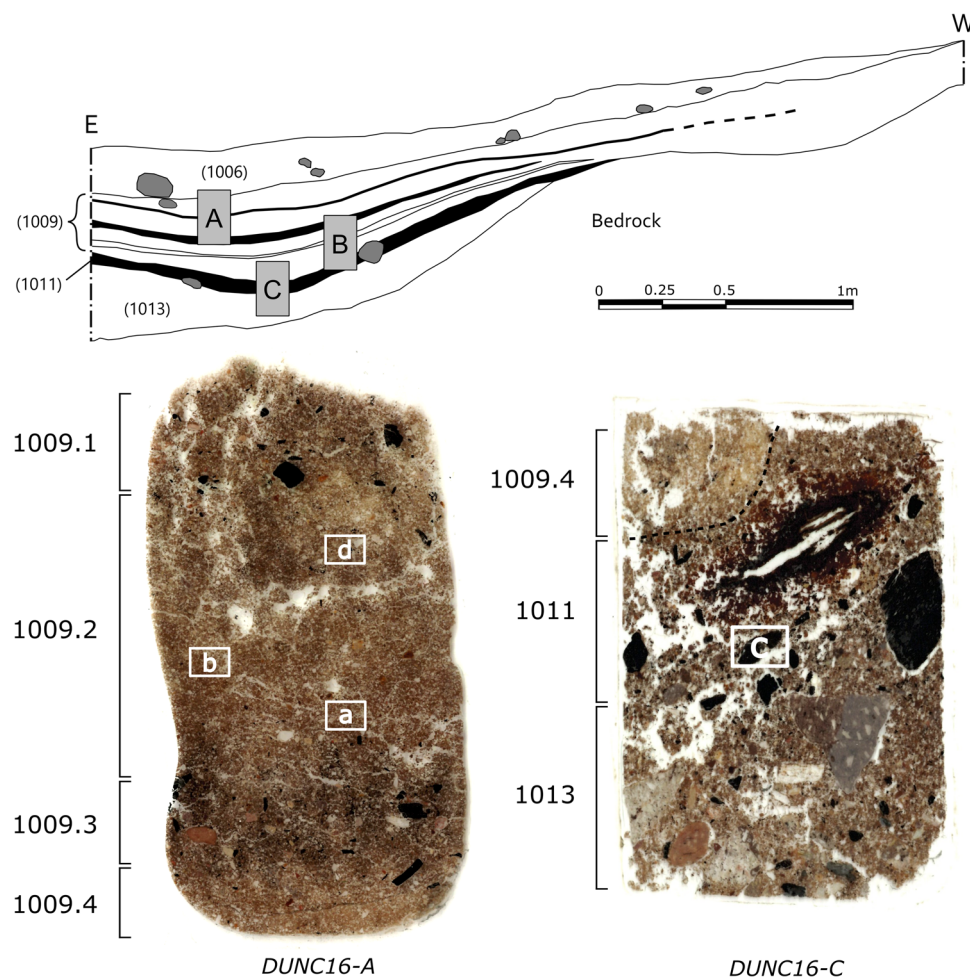
FIGURE 15 Scans of Dunnicaer thin sections DUNC16-A (left) and DUNC16-C (right), with section drawing (top) showing sampled stratigraphy, subcontexts of 1009 and location of photomicrographs in Figure 16.

to the understanding of the plan of the structure, suggesting that it was approximately 8 m in length and 5 m in width, with a straight end wall on the southeast and a rounded northwest end. This form is similar to the heel-shaped building found at Portmahomack, a high-status early medieval settlement and monastery in northern Scotland (Carver, 2016, p. 134; Carver et al., 2016, pp. 228–246). The Portmahomack structure appeared to be constructed with a turf wall and wattle cladding and was interpreted as a craft workshop that had at least two phases of the use—the first during the 8th century and the second in the 9th/10th centuries, when it was converted into a grain-drying kiln (Carver et al., 2016, p. 235).

There is little evidence to suggest the function or status of Burghead Building 2, other than a rotary quern stone, and its location towards the seaward end of the upper citadel, which is assumed to be the higher status part of the settlement. Recent excavations have uncovered a concentration of workshops with bone and shell middens in the lower citadel, where the volume of material contrasts with the limited artefactual and faunal

record recovered from the 2015–2017 trenches. This contrast alone may suggest that Building 2 had a more domestic function; however, preservation was considerably better in the lower citadel, and additional post-depositional factors affecting Building 2 (truncation, stone robbing and possible reuse) are likely to have exacerbated this difference. It is also possible that upper citadel buildings were kept cleaner and/or were more thoroughly robbed of materials at the end of their life, and that this may have been related to a higher status. Indeed, a large pit with midden-like material (Figure 18) at the northern side of the building contrasts with the above-ground middens that occur on the lower citadel.

Extensive bioturbation and eluviation meant that it was not possible to convincingly identify 105 or 106 as floor layers in thin section, with many of the characteristic properties (microstratigraphy, planar voids, compaction and horizontal distributions) being completely absent (Milek, 2012; Rentzel et al., 2017). In this instance, recognition of them as occupation deposits was achieved primarily through the spatial geochemistry results,

TABLE 6 Summary of descriptive sediment attributes, inclusions and post-depositional alterations at Dunnicaer.

Slide/unit	Structure — Textural class	Structure — Microstructure	Course:fine (100 μm) ratio	Void types[a] — Channels and vughs	Void types[a] — Planar (random)	Void types[a] — Planar (horizontal)	Void types[a] — Compound packing voids	Fine material — Nature of fine material (PPL)	Fine material — Colour of fine material (OIL)	Fine material — Birefringence fabric (XPL)
A1009.1	Sandy silt loam	Weakly to moderately developed subangular blocky with channels	55:45	■■■■■■■■	■■■			Orangish-brown; dotted	Orangish-yellow	Stipple-speckled
A1009.2	Sandy silt loam	Moderately developed subangular blocky with channels and horizontal planar voids	40:60	■■■■■■■	■■■	■■■■	■	Orangish-brown; mid-brown; dotted	Orangish-yellow; brownish-yellow	Stipple-speckled
A1009.3	Organic sandy silt loam	Well-developed subangular blocky with intra-aggregate crumb structure and channels	35:65	■■■■■■	■■■■■■	■	■■■	Orangish-brown; dark brown; dotted	Yellowish-brown; dark brown	Stipple-speckled; localised undifferentiated
B1009.4	Sandy silt loam	Moderately to well-developed subangular blocky with intra-aggregate crumb structure and channels	35:65	■■■■■	■■■■■■■		■■■	Orangish-brown; dark brown; dotted	Yellowish-orange; dark brown	Stipple-speckled
C1011	Organic silt loam	Crumb with localised channels	55:45	■■■■	+		■■■■■■■■■	Orangish-brown; dark brown; dotted	Brownish-yellow; dark brown	Stipple-speckled
C1013	Sandy silt loam	Channels with localised subangular blocky structure	65:35	■■■■■■■■■	■■			Orangish-brown; dotted	Brownish-yellow	Stipple-speckled

Slide/unit	Organic matter — Charred	Organic matter — Uncharred	Inclusions — Intrusive aggregates	Inclusions — Rubified fine material	Pedofeatures — Fe/Mn	Pedofeatures — Excremental
A1009.1	■■■■	■■■		■	■	■■
A1009.2	■	■■■	+	+	■	■■
A1009.3	■■■	■■■			■	■
B1009.4	■	■■■	+	+	+	■
C1011	■■■■	■■■			■■■■■	■■■
C1013	■■	■		■	■	■■

Abbreviations: +, present in trace amounts; ■, <2%; ■■, 2%–5%; ■■■, 5%–10%; ■■■■, 10%–20%; ■■■■■, 20%–30%; ■■■■■■, 30%–40%; ■■■■■■■, 40%–50%; ■■■■■■■■, 50%–60%; ■■■■■■■■■, 60%–70%; ■■■■■■■■■■, >70%.

[a]Void frequency refers to % total void space (following Bullock et al., 1985; Stoops, 2021, p. 73).
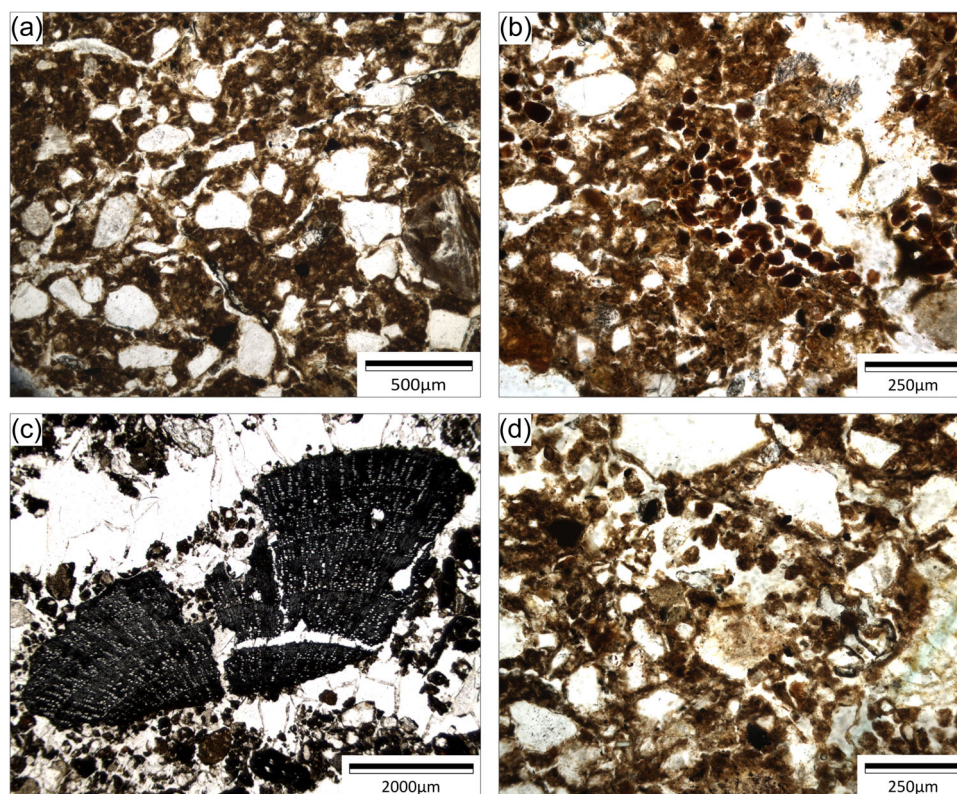
FIGURE 16 Photomicrographs (plane-polarised light [PPL]) of Dunnicaer thin sections, (a) DUNC16-A, context 1009.2, showing a subangular blocky microstructure and horizontal planar voids in a relict floor; (b) DUNC16-A, context 1009.2, showing heavily degraded organic nodules; (c) DUNC16-C, context 1011, showing a 9 y/o hazel charcoal fragment; and (d) DUNC16-A, context 1009.2, showing excremental pedofeatures in channel as evidence of bioturbation.

mirroring the findings of the comparative geoarchaeological study on the broadly contemporary Pictish building at Lair (Reid et al., 2023). However, micromorphology was able to clarify the composition of the Burghead layers and demonstrated the presence and survival of anthropogenic material. The overall issues identified at Burghead are therefore similar to those of urban dark earths—a term used to refer to thick, poorly stratified, dark-coloured, non-peaty deposits that contain anthropogenic material (Nicosia et al., 2017, p. 331). The homogeneous appearance of dark earths means that they provide little archaeological detail at a macroscopic scale, and soil micromorphology is often successfully used to understand the type and rate of the processes involved in their formation (e.g., bioturbation, chemical weathering, agriculture and anthropogenic dumping and mixing) (Borderie et al., 2015; Cremaschi & Nicosia, 2010; Devos, Nicosia, et al., 2013; Devos, Wouters, et al. 2013; Macphail, 1994, 2014). Dark earths challenge the traditional concept of 'one stratigraphic unit equals one action' (Harris, 1989) and the stratigraphy at Burghead appears to represent these processes as well (Nicosia et al., 2017, p. 339). This suggests that the same methodological and theoretical principles applied to dark earths (see Borderie et al., 2015; Macphail et al., 2003; Nicosia et al., 2017) should also be applied to other poorly stratified occupation deposits.

5.2 | Dunnicaer

The northeast corner of the Dunnicaer trench returned a markedly higher quantity of burnt bone than observed elsewhere across the sampled area (Figure 19). Given its proximity to the hearth, it is most likely that the cluster resulted from the deliberate dumping of hearth waste, although the comparatively low magnetism and limited quantity of charcoal might suggest that larger bones and bone fragments were picked out and placed there, rather than being swept up together with ash and charcoal residues. More generally, there was a broad correlation between the highest concentration of elements and the highest quantity of bone and charcoal microrefuse. The most obvious suggestion is that the hearth residues were the primary contributor to geochemical signatures; however, it is also possible that they acted concurrently as element traps and archives. Previous studies have demonstrated that the preservation potential of certain elements is dependent on the presence/absence of fixing agents (such as bone and charcoal) that can retain and even uptake levels of Ca, P, Sr, Zn and Cu (Davidson et al., 2007; Wilson et al., 2006, 2008). Bone distribution correlates most closely with Ca, Sr, Zn, and to some extent Cu and Mg, and would appear to provide further support for this finding.
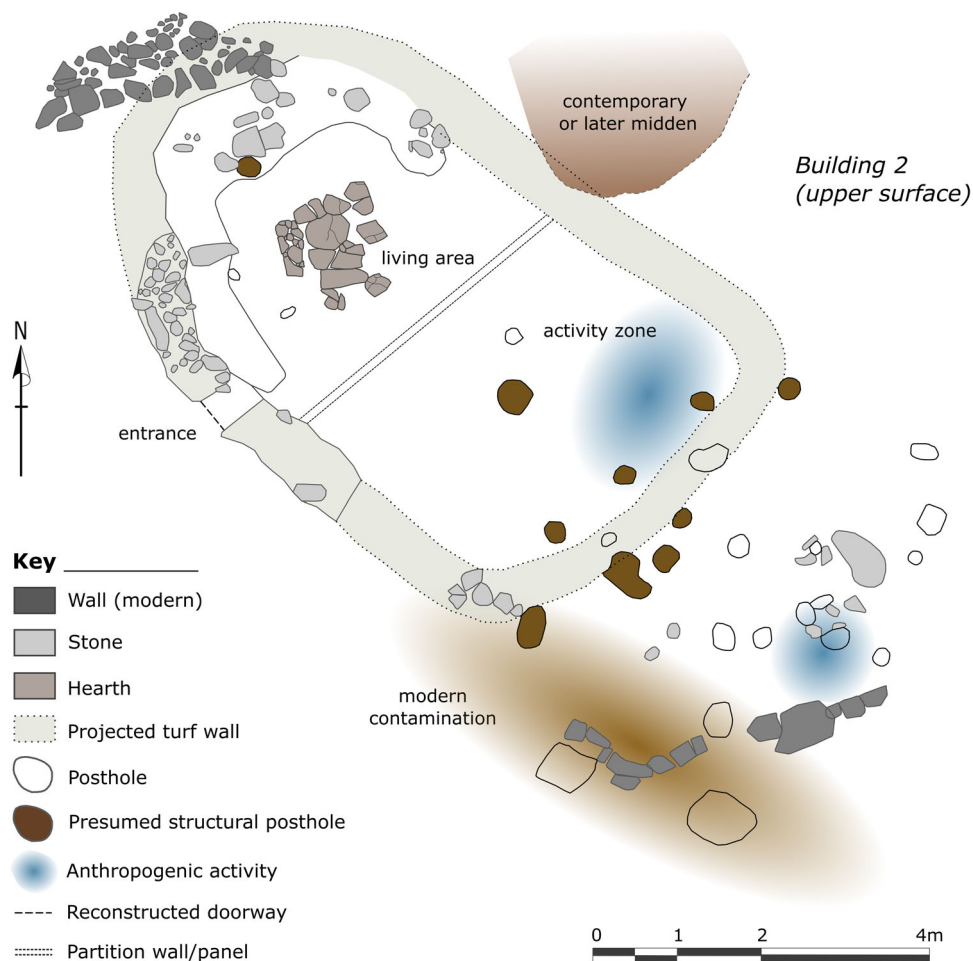
FIGURE 17 Interpretive plan of Burghead upper surface, based on integrated field, microrefuse, geochemical and micromorphological evidence.

The increased organic content identified in the southwest corner of the trench has no clear source but may be attributable to turf wall construction that has since degraded and slumped over onto the hearth rake-out, perhaps resulting in a commingled organic/magnetic signature (Figure 19). Its proximity to the bedrock could suggest that the structure utilised the exposed geology on the eastern side of the trench as part of the wall for the structure. If so, this would provide rare evidence for construction, as definitive traces of outer walling and postholes were only identified in association with one other structure on the fort (Noble et al., 2020).

The difference in magnetic signatures observed between the upper hearth and the area of context 1007 supports the latter's interpretation as hearth rake-out (Figure 19; Noble et al., 2020, p. 283). It would also suggest that this extended further towards the south of the trench than was visible in the field. The elevation of P, Mn and Zn within the hearth—and P and Mn within the rake-out—suggests that dung may have supplemented the fuel source, with the geoarchaeological study at Lair identifying enrichment of these elements in the area of an early medieval longhouse believed to

house animals (Reid et al., 2023). Magnetic signatures could also have resulted from the use of wood ash mixed with heated soil material from the base of the hearth or soil-rich fuel sources such as turf or peat (although characteristic evidence for the latter was missing both in the field and in thin section). Micromorphological work at the Iron Age Clachtoll Broch has confirmed the presence of wood, peat and dung within a single hearth, and recognised that the use of fuel types changed frequently, perhaps reflecting seasonal changes depending on availability (Roy, 2022). The presence of burnt animal bones and the enrichment of Ca within the hearth deposits at Dunnicaer suggest that the upper hearth on the lower terrace primarily served a domestic function related to food preparation and consumption, rather than being associated with craft or metalworking.

The presence of charcoal-rich lenses either side of a thicker trampled layer may be suggestive of a maintenance practice that involved the treatment or sealing of well-worn floor deposits with ash. Both wood ash (calcium carbonate) and faecal spherulites (present in animal dung) dissolve rapidly when exposed to rainwater; thus, their absence in the free-draining soils at
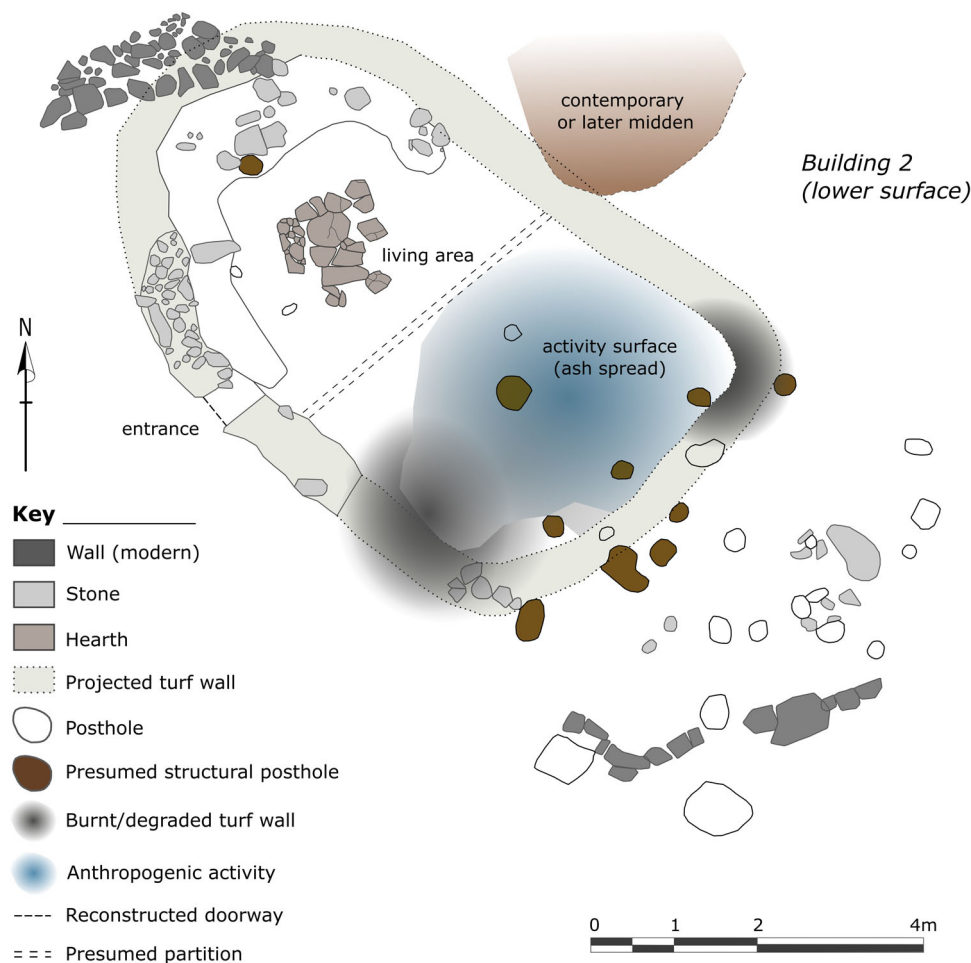
FIGURE 18 Interpretive plan of Burghead lower surface, based on integrated field, microrefuse, geochemical and micromorphological evidence.

Dunnicaer is unsurprising (Braadbaart et al., 2017; Canti, 2003; Canti & Brochier, 2017a, 2017b; Karkanas, 2021). Interestingly, remnants of ash-spreading were more apparent in thin section than in the spatial distribution maps, providing a notable contrast to the findings at Burghead. This is convincing evidence that the deposit targeted for grid sampling was the floor layer 1009.2 and that the geochemical results are therefore representative of a repeatedly trampled activity surface.

The rebuilding lens (1009.4) and shallow floor deposit (1011) identified in relation to the lower hearth likely indicate the removal of cumulative layers before the building of the new hearth, reflecting a pattern of reuse observed more widely at Dunnicaer. Multiple rebuilding episodes in the upper terrace were evidenced by superimposed hearths, structures and features, suggesting that structures were built, repaired and replaced while retaining similar ground plans (Noble et al., 2020, p. 277). This has been interpreted as a response to intense activity on the site and rapid expansion of the settlement over a relatively limited area (Noble et al., 2020, p. 320). The removal of previous occupation deposits is therefore an important consideration in structures where occupation deposits are thin or fragmentary. Microlaminations containing

more nuanced evidence of domestic activity are likely to have been removed, truncated or disrupted through these cleaning events (see Milek, 2012, p. 134). Again, this challenges the concept that a single stratigraphic unit represents a single activity. Maintenance practices are part of the fabric of daily life, and it is therefore misleading to equate thin or homogeneous stratigraphy with an absence of evidence for settlement activity.

5.3 | Evaluation of the integrated geoarchaeological approach

The results presented above illustrate the value in conducting multi-method, integrated geoarchaeological approaches on poorly preserved and fragmented archaeological sites. At Burghead, PCA and multi-element by pXRF were able to establish the soil element profile for an area of known contamination in the upper surface, allowing the 'noise' from the affected area to be effectively filtered out. This enabled the recognition of more 'authentic' patterns of enrichment but needed to be undertaken in relation to microrefuse analysis and the presence/absence of industrial waste.
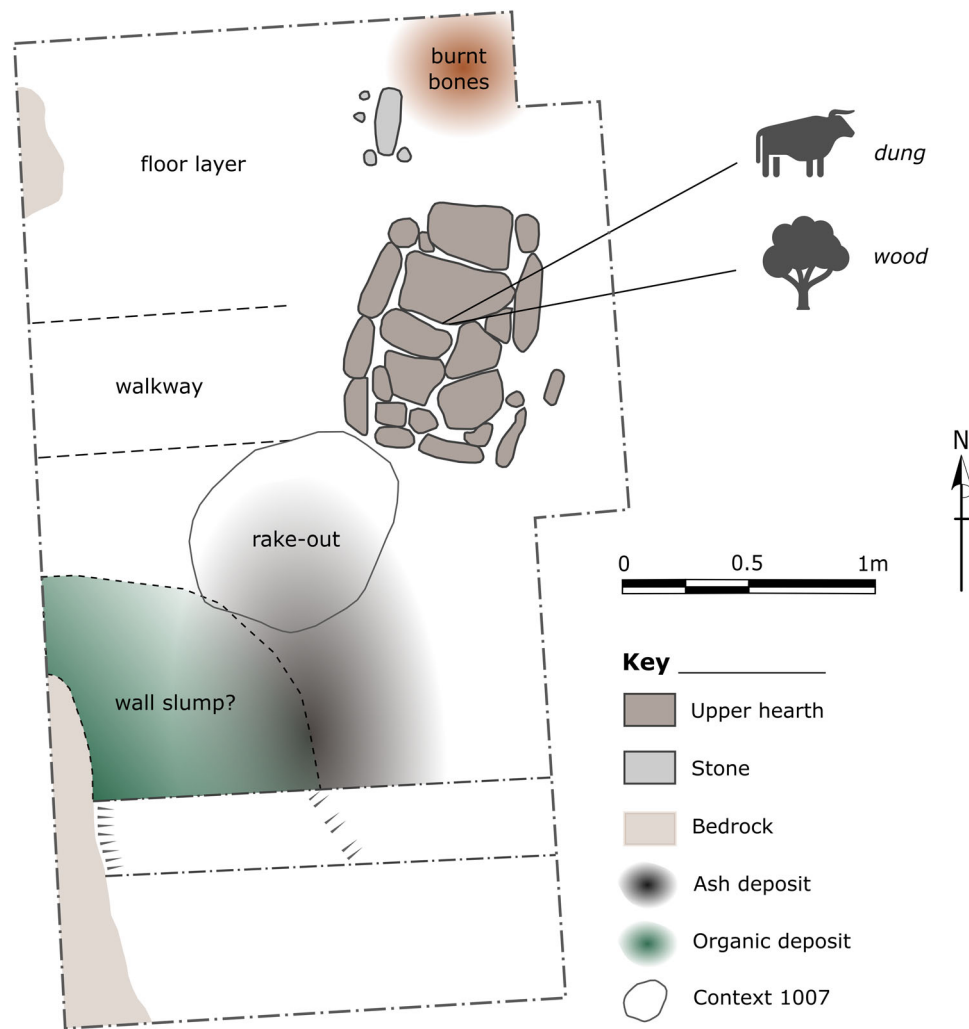
FIGURE 19 Interpretive plan of Dunnicaer lower terrace structure, based on integrated field, microrefuse, geochemical and micromorphological evidence. For interpretation of the colour in this figure and legend, the reader is referred to the web version of this article.

Results from Dunnicaer have indicated that element concentrations are partly related to the presence/absence of fixing agents, suggesting that certain anthropogenic signatures are more resistant and may persist in soil for relatively long periods of time in comparison with other elements that can leach more rapidly (Wilson et al., 2008, p. 423). Variations in pH also affect chemical processes such as bioavailability and vulnerability to leaching; however, the narrow range of soil pH values observed at both sites indicates that the elemental variations are largely due to other factors, such as anthropogenic deposition (Entwistle et al., 1998, pp. 63–64). The interpretation of multi-element results should therefore always be made in comparison to data on the concentration of other elements and microrefuse, as well as pH, which will affect the survival of different element types and fixing agents such as bone (Milek & Roberts, 2013, p. 1863).

On its own, micromorphology provided clear evidence for the post-depositional processes affecting the sites. In the better-preserved stratigraphy at Dunnicaer, micromorphology was able to detect discrete depositional events and evidence for remodelling before the construction of the upper hearth. Moreover, it was able to identify areas of

surviving microstructure and filter out the effects of bioturbation—a feat not achievable in the field or through chemical survey. Extensive illuviation and near complete bioturbation of the archaeological stratigraphy at Burghead meant that floor layers were not readily identifiable in thin section; however, one of the block samples (BHF16-A) did capture an area of unique preservation not recognised during excavation that provided detail regarding structure construction and/or destruction. It is also very promising that surviving characteristics of the use of space were present in the geochemical, magnetic and elemental data, even when floor layers were not preserved in thin section. This mirrors recent findings at the site of Lair, in Perthshire, where floor layers were very thin, fragmentary and had been affected by bioturbation but revealed clear pattering in geochemistry and magnetic susceptibility (Reid et al., 2023). It was also hypothesised that maintenance practices and the use of floor coverings may have contributed to their limited recovery, as these practices can remove occupation evidence and prevent the build-up and trampling of material (Reid et al., 2023). Indeed, building 1 at Burghead (Figure 3) appears to contain evidence for a suspended wooden floor and the practice may be

more widespread than is currently realised. The results of these studies have therefore demonstrated the value in conducting geoarchaeological investigation on fragmented or poorly preserved buildings but also the need for integrated approaches, rather than a reliance on individual techniques.

6 | CONCLUSION

The integrated geoarchaeological methodologies presented in this study have proven fundamental to the assessment of preservation, site activities and post-depositional events at two fragmented structures in northeast Scotland. They have helped clarify the outline and dimensions of a poorly preserved building at Burghead, and provided new layers of detail that have enriched our understanding of daily life in first millennium A.D. coastal settlements, including wattle-and-daub construction, possible partitioning of space, interior remodelling and the use of dung as a fuel source. The indication that both buildings served a domestic function supports field interpretations and enables the reconstruction of site organisation, particularly in the larger fort at Burghead, where ongoing excavations are uncovering workshops and middens situated away from these structures. The use of overlapping microrefuse and geochemical data sets, correlation tables and PCA greatly enhanced the interpretational power of individual techniques and were key to recognising the impacts of post-medieval contamination and biases in the survival of different element types. Integrating these bulk soil analyses with soil micromorphological analysis then enabled the recognition of floor layers and maintenance practices, providing key detail about the survival, composition and compaction of the identified occupation deposits.

This study has therefore demonstrated that geoarchaeology can play a significant role in elucidating the original composition and spatial patterning of highly fragmented buildings and occupation surfaces. Evidence survives in the micro-residues deposited by human activity and can be meaningfully linked to the practices that governed everyday life. This study has also shown the need to consider the post-depositional processes that can affect the integrity of occupation surfaces at the macroscale, and highlights the pitfalls associated with equating thin or homogeneous stratigraphy with an absence of evidence for settlement activity. Doing so will not only omit crucial information but also risk creating less reliable interpretations of archaeological structures and their assemblages. Though this study has presented the results from early medieval sites in Scotland, it offers an integrated methodology and theoretical principle that can be applied to fragmented buildings and occupation deposits around the world.

AUTHOR CONTRIBUTIONS

Vanessa Reid: Conceptualisation; methodology; formal analysis; investigation; writing—original draught; writing—review and editing; visualisation. **Karen Milek**: Conceptualisation; methodology; writing—review and editing; supervision; funding acquisition. **Charlotte O'Brien**: Investigation. **Óskar G. Sveinbjarnarson**: Resources. **Gordon Noble**: Funding acquisition; writing—review and editing.

CONFLICT OF INTEREST STATEMENT

The authors declare no conflict of interest.

DATA AVAILABILITY STATEMENT

The data that support the findings of this study are available in the supplementary material of this article.

ORCID

Vanessa Reid http://orcid.org/0000-0002-4399-9390

REFERENCES

Alcock, L. (2003). *Kings and warriors, craftsmen and priests in northern Britain AD 550-850*. Society of Antiquaries of Scotland.

Banerjea, R. Y., Bell, M., Matthews, W., & Brown, A. (2015). Applications of micromorphology to understanding activity areas and site formation processes in experimental hut floors. *Archaeological and Anthropological Sciences*, 7, 89–112.

Benton, M. J., Cook, E., & Turner, P. (2002). *Permian and triassic red beds and the Penarth Group of Great Britain*. Joint Nature Conservation Committee.

BGS. (2022). *BGS geology viewer*. https://www.bgs.ac.uk/map-viewers/bgs-geology-viewer/

Bintliff, J., & Degryse, P. (2022). A review of soil geochemistry in archaeology. *Journal of Archaeological Science: Reports*, 43, 103419.

Borderie, Q., Ball, T., Banerjea, R., Bizri, M., Lejault, C., Save, S., & Vaughan-Williams, A. (2020). Early middle ages houses of Gien (France) from the inside: Geoarchaeology and archaeobotany of 9th–11th c. floors. *Environmental Archaeology*, 25, 151–169.

Borderie, Q., Devos, Y., Nicosia, C., Cammas, C., & Macphail, R. I. (2015). Dark earth in the geoarchaeological approach to urban contexts. In N. Carcaud & G. Arnaud-Fassetta (Eds.), *La géoarchéologie française au XXIE siècle* (pp. 245–255). CNRS Éditions.

Braadbaart, F., van Brussel, T., van Os, B., & Eijskoot, Y. (2017). Fuel remains in archaeological contexts: Experimental and archaeological evidence for recognizing remains in hearths used by Iron Age farmers who lived in peatlands. *The Holocene*, 27, 1682–1693.

Bullock, P., Fedoroff, N., Jongerius, A., Stoops, G., Tursina, T., & Babel, U. (1985). *Handbook for soil thin section description*. Waine Research Publications.

Cannell, R. J. S. (2012). On the definition and practice of geoarchaeology. *Primitive Tider*, 14, 31–46.

Canti, M. G. (2003). Aspects of the chemical and microscopic characteristics of plant ashes found in archaeological soils. *Catena*, 54, 339–361.

Canti, M. G., & Brochier, J. E. (2017a). Faecal spherulites. In C. Nicosia & G. Stoops (Eds.), *Archaeological soil and sediment micromorphology* (pp. 47–50). John Wiley & Sons.

Canti, M. G., & Brochier, J. E. (2017b). Plant ash. In C. Nicosia & G. Stoops (Eds.), *Archaeological soil and sediment micromorphology* (pp. 147–154). John Wiley & Sons.

Carver, M. (2016). *Portmahomack: Monastery of the picts* (2nd ed.). Edinburgh University Press.

Carver, M., Garner-Lahire, J., & Spall, C. (2016). *Portmahomack on tarbat ness: Changing ideologies in north-east Scotland, sixth to sixteenth century AD*. Society of Antiquaries of Scotland.

Courty, M. A., Goldberg, P., & Macphail, R. (1989). *Soils and micromorphology in archaeology*. Cambridge University Press.

Cremaschi, M., & Nicosia, C. (2010). Corso Porta Reno, Ferrara (Northern Italy): A study in the formation processes of urban deposits. *Il Quaternario—Italian Journal of Quaternary Sciences*, 23, 395–408.

Croffie, M. E. T., Williams, P. N., Fenton, O., Fenelon, A., & Daly, K. (2022). Rubidium measured by XRF as a predictor of soil particle size in limestone and siliceous parent materials. *Journal of Soils and Sediments*, 22, 818–830.

Davidson, D. A., Wilson, C. A., Meharg, A. A., Deacon, C., & Edwards, K. J. (2007). The legacy of past manuring practices on soil contamination in remote rural areas. *Environment International*, 33, 78–83.

Dearing, J. (1999). *Environmental magnetic susceptibility: Using the Bartington MS2 system* (2nd ed.). Bartington Instruments.

Devos, Y., Nicosia, C., Vrydaghs, L., & Modrie, S. (2013). Studying urban stratigraphy: Dark earth and a microstratified sequence on the site of the Court of Hoogstraeten (Brussels, Belgium). Integrating archaeopedology and phytolith analysis. *Quaternary International*, 315, 147–166.

Devos, Y., Vrydaghs, L., Collette, O., Hermans, R., & Loicq, S. (2022). Understanding the formation of buried urban anthrosols and technosols: An integrated soil micromorphological and phytolith study of the dark earth on the Mundaneum site (Mons, Belgium). *Catena*, 215, 106322.

Devos, Y., Wouters, B., Vrydaghs, L., Tys, D., Bellens, T., & Schryvers, A. (2013). A soil micromorphological study on the origins of the early medieval trading centre of Antwerp (Belgium). *Quaternary International*, 315, 167–183.

Driscoll, S. T. (1997). Pictish settlement in north-east Fife: The Scottish Field School of Archaeology Excavations at Easter Kinnear. *Tayside and Fife Archaeological Journal*, 3, 74–118.

Driscoll, S. T. (2011). Pictish archaeology: Persistent problems and structural solutions. In S. T. Driscoll, J. Geddes, & M. A. Hall (Eds.), *Pictish progress: New studies on Northern Britain in the early middle ages* (pp. 245–280). Brill.

Dunwell, A., & Ralston, I. B. M. (2008). *Archaeology and early history of Angus*. The History Press.

Edwards, K. J., & Ralston, I. (1980). New dating and environmental evidence from Burghead Fort, Moray. *Proceedings of the Society of Antiquaries of Scotland*, 109, 202–210.

Entwistle, J. A., Abrahams, P. W., & Dodgshon, R. A. (1998). Multi-element analysis of soils from Scottish historical sites: Interpreting land-use history through the physical and geochemical analysis of soil. *Journal of Archaeological Science*, 25, 53–68.

Entwistle, J. A., McCaffrey, K. J. W., & Dodgshon, R. A. (2007). Geostatistical and multi-elemental analysis of soils to interpret land-use history in the Hebrides, Scotland. *Geoarchaeology*, 22, 391–415.

Farnham, I. M., Singh, A. K., Stetzenbach, K. J., & Johannesson, K. H. (2002). Treatment of nondetects in multivariate analysis of groundwater geochemistry data. *Chemometrics and Intelligent Laboratory Systems*, 60, 265–281.

Fenton, A. (1978). *The Northern Isles: Orkney and Shetland*. John Donald Publishers.

Fitzpatrick, E. A. (1984). *Micromorphology of soils*. Chapman and Hall.

Foster, S. M. (2014). *Picts, Gaels and Scots*. Birlinn.

French, C. (2015). *A handbook of geoarchaeological approaches for investigating landscapes and settlement sites*. Oxbow Books.

Friesem, D. E., Wattez, J., & Onfray, M. (2017). Earth construction materials. In C. Nicosia & G. Stoops (Eds.), *Archaeological soil and sediment micromorphology* (pp. 99–110). John Wiley & Sons.

Garcia, D., Fonteilles, M., & Moutte, J. (1994). Sedimentary fractionations between Al, Ti and Zr and the genesis of strongly peraluminous granites. *The Journal of Geology*, 102, 411–422.

Gardner, T. (2018). *The geoarchaeology of burnt mounds: Site formation processes, use patterns, and duration*. University of Edinburgh.

Goldberg, P. (1988). Commentary: The archaeologist as viewed by the geologist. *The Biblical Archaeologist*, 51, 197–202.

Goldberg, P. (2008). Raising the bar: Making geological and archaeological data more meaningful for understanding the archaeological record. In A. P. Sullivan III (Ed.), *Archaeological concepts for the study of the cultural past* (pp. 24–39). University of Utah Press.

Goldberg, P., & Aldeias, V. (2018). Why does (archaeological) micromorphology have such little traction in (geo)archaeology? *Archaeological and Anthropological Sciences*, 10, 269–278.

Harris, E. C. (1989). *Principles of archaeological stratigraphy*. Academic Press.

Huisman, D. J. (Ed.). (2009). *Degradation of archaeological remains*. Sdu Uitgevers.

Jones, R., Challands, A., French, C., Card, N., Downes, J., & Richards, C. (2010). Exploring the location and function of a Late Neolithic house at Crossiecrown, Orkney by geophysical, geochemical and soil micromorphological methods. *Archaeological Prospection*, 17, 29–47.

Kaiser, H. F. (1960). The application of electronic computers to factor analysis. *Educational and Psychological Measurement*, 20, 141–151.

Kaiser, H. F. (1970). A second generation Little Jiffy. *Psychometrika*, 35, 401–415.

Karkanas, P. (2021). All about wood ash: Long term fire experiments reveal unknown aspects of the formation and preservation of ash with critical implications on the emergence and use of fire in the past. *Journal of Archaeological Science*, 135, 105476.

Karkanas, P., & Goldberg, P. (2016). Soil micromorphology. In A. S. Gilbert, P. Goldberg, V. T. Holliday, R. D. Mandel, & R. S. Sternberg (Eds.), *Encyclopedia of geoarchaeology* (pp. 830–841). Springer.

Kibblewhite, M., Tóth, G., & Hermann, T. (2015). Predicting the preservation of cultural artefacts and buried materials in soil. *Science of the Total Environment*, 529, 249–263.

Kidder, T. R., Kai, S., Henry, E. R., Grooms, S. B., & Ervin, K. (2021). Multi-method geoarchaeological analyses demonstrates exceptionally rapid construction of Ridge West 3 at Poverty Point. *Southeastern Archaeology*, 40, 212–227.

Knudson, K. J., Frink, L., Hoffman, B. W., & Price, T. D. (2004). Chemical characterization of Arctic soils: Activity area analysis in contemporary Yup'ik fish camps using ICP-AES. *Journal of Archaeological Science*, 31, 443–456.

Kooistra, M. J., & Pulleman, M. M. (2018). Features related to faunal activity. In G. Stoops, V. Marcelino, & F. Mees (Eds.), *Interpretation of micromorphological features of soils and regoliths* (2nd ed., pp. 447–469). Elsevier.

Kühn, P., Aguilar, J., Miedema, R., & Bronnikova, M. (2018). Textural pedofeatures and related horizons. In G. Stoops, V. Marcelino, & F. Mees (Eds.), *Interpretation of micromorphological features of soils and regoliths* (2nd ed., pp. 377–424). Elsevier.

Kwak, S. G., & Kim, J. H. (2017). Central limit theorem: The cornerstone of modern statistics. *Korean Journal of Anesthesiology, 70*, 144–156.

LaMotta, V. M., & Schiffer, M. B. (1999). Formation processes of house floor assemblages. In P. M. Allison (Ed.), *The archaeology of household activities* (pp. 19–29). Routledge.

Lehmann, J., & Schroth, G. (2003). Nutrient leaching. In G. Schroth & F. L. Sinclair (Eds.), *Trees, crops and soil fertility: Concepts and research methods* (pp. 151–166). CABI Publishing.

Lewis, H. (2023). Archaeological soil micromorphology. In M. Pollard, R. A. Armitage, & C. Makarewicz (Eds.), *Handbook of archaeological sciences* (2nd ed., pp. 253–269). Wiley.

Macdonald, J. (1862). Historical notices of the 'Broch' or Burghead, in Moray, with an account of its antiquities. *Proceedings of the Society of Antiquaries of Scotland, 4*, 321–342.

Macphail, R. I. (1994). The reworking of urban stratigraphy by human and natural processes. In A. R. Hall & H. K. Kenward (Eds.), *Urban-rural connexions: Perspectives from environmental archaeology. Symposia of the Association for Environmental Archaeology No. 12, Oxbow Monograph* (47, pp. 13–43). Oxbow Books.

Macphail, R. I. (2014). Reconstructing past land use from dark earth: Examples from England and France. In E. Lorans & X. Rodier (Eds.), *Archéologie de l'Espace Urbain* (pp. 251–261). Presses Universitaires François Rabelais.

Macphail, R. I., Galinié, H., & Verhaeghe, F. (2003). A future for dark earth? *Antiquity, 77*, 349–358.

Macphail, R. I., & Goldberg, P. (2018). *Applied soils and micromorphology in archaeology*. Cambridge University Press.

McGill, C. (2004). Excavations of cropmarks at Newbarns, near Inverkeilor, Angus. *Tayside and Fife Archaeological Journal, 10*, 94–118.

Mentzer, S. M., & Quade, J. (2013). Compositional and isotopic analytical methods in archaeological micromorphology. *Geoarchaeology, 28*, 87–97.

Milek, K. B. (2012). Floor formation processes and the interpretation of site activity areas: An ethnoarchaeological study of turf buildings at Thverá, northeast Iceland. *Journal of Anthropological Archaeology, 31*, 119–137.

Milek, K. B., & French, C. A. I. (2007). Soils and sediments in the settlement and harbour at Kaupang. In D. L. Skre (Ed.), *Kaupang in skiringssal* (pp. 321–360). Aarhus University Press.

Milek, K. B., & Roberts, H. M. (2013). Integrated geoarchaeological methods for the determination of site activity areas: A study of a Viking Age house in Reykjavik, Iceland. *Journal of Archaeological Science, 40*, 1845–1865.

Milek, K., Heron, C., Armitage, R. A., & Manoukian, N. (2023). Geochemical prospection and the identification of site activity areas. In M. Pollard, R. A. Armitage, & C. Makarewicz (Eds.), *Handbook of archaeological sciences* (2nd ed., pp. 1025–1044). Wiley.

Nesbitt, C., Church, M. J., Gilmour, S. M. D., & Burgess, C. P. G. (2013). Small-scale evaluation of a post-medieval blackhouse at Bereiro, Lewis, Western Isles of Scotland. *Journal of the North Atlantic, 5*, 1–19.

Nicosia, C., Devos, Y., & Macphail, R. I. (2017). European dark earths. In C. Nicosia & G. Stoops (Eds.), *Archaeological soil and sediment micromorphology* (pp. 331–343). John Wiley & Sons.

Nicosia, C., & Stoops, G. (Eds.). (2017). *Archaeological soil and sediment micromorphology*. John Wiley & Sons.

Nielsen, N. H., & Kristiansen, S. M. (2014). Identifying ancient manuring: Traditional phosphate vs. multi-element analysis of archaeological soil. *Journal of Archaeological Science, 42*, 390–398.

Noble, G., & Evans, N. (2022). *Picts: Scourge of Rome, rulers of the north*. Birlinn.

Noble, G., Evans, N., Hamilton, D., MacIver, C., Masson-MacLean, E., & O'Driscoll, J. (2020). Dunnicaer, Aberdeenshire, Scotland: A Roman Iron Age promontory fort beyond the frontier. *Archaeological Journal, 177*, 256–338.

Noble, G. (2019). Fortified settlement in northern Pictland. In G. Noble & N. Evans (Eds.), *The king in the north* (pp. 39–57). Birlinn.

Noble, G., Gondek, M., Campbell, E., Evans, N., Hamilton, D., & Taylor, S. (2019). A powerful place of Pictland: Interdisciplinary perspectives on a power centre of the 4th to 6th centuries AD. *Medieval Archaeology, 63*, 56–94.

Noble, G., MacIver, C., Masson-Maclean, E., & O'Driscoll, J. (2018). *Burghead 2018: Dating the enclosing elements and characterizing the survival and use of the lower citadel*. University of Aberdeen.

Oram, R. (2007). Capital tales or Burghead bull? In S. Arbuthnot & K. Hollo (Eds.), *Fil Súil nGlais: A grey eye looks back: A festschrift in honour of colm Ó Baoill* (pp. 241–262). Clann Tuirc.

Ottaway, J. H., & Matthews, M. R. (1988). Trace element analysis of soil samples from a stratified archaeological site. *Environmental Geochemistry and Health, 10*, 105–112.

Parker Pearson, M., & Richards, C. (Eds.). (1994). *Architecture and order: Approaches to social space*. Routledge.

Ralston, I. B. M. (2006). *Excavations on behalf of the Burghead Headland Trust within the fort of Burghead, Moray, September 2003: An interim statement*. https://www.ianralston.co.uk/projects.html

Reid, V. (2021). A process of elimination? Reviewing the fragmented settlement record of eastern Pictland and its implications for future research. *Medieval Settlement Research, 36*, 49–60.

Reid, V., & Milek, K. (2021). Risk and resources: An evaluation of the ability of national soil datasets to predict post-depositional processes in archaeological sites and heritage at risk. *Heritage, 4*, 725–758.

Reid, V., Milek, K., O'Brien, C., Sneddon, D., & Strachan, D. (2023). Revealing the invisible floor: Integrated geoarchaeological analyses of ephemeral occupation surfaces at an early medieval farmhouse in upland Perthshire, Scotland. *Journal of Archaeological Science, 159*, 105825. https://doi.org/10.1016/j.jas.2023.105825

Reidsma, F. H., Sifogeorgaki, I., Dinckal, A., Huisman, H., Sier, M. J., van Os, B., & Dusseldorp, G. L. (2021). Making the invisible stratigraphy visible: A grid based, multi-proxy geoarchaeological study of Umhlatuzana Rockshelter, South Africa. *Frontiers in Earth Science, 9*, 664105.

Rentzel, P., Nicosia, C., Gebhardt, A., Brönnimann, D., Pümpin, C., & Ismail-Meyer, K. (2017). Trampling, poaching and the effect of traffic. In C. Nicosia & G. Stoops (Eds.), *Archaeological soil and sediment micromorphology* (pp. 281–297). John Wiley & Sons.

Robertson, J., & Roy, L. M. (2021). A Scottish Iron Age wetland village built from nature's bounty: Understanding the formation of plant litter floors. *Environmental Archaeology, 26*, 222–237.

Rowell, D. L. (1994). *Soil science: Methods and applications*. Longman.

Roy, L. (2022). The floor and internal deposits: Soil micromorphology. In G. Cavers (Ed.), *Clachtoll: An Iron Age Broch settlement in Assynt, North-west Scotland* (pp. 282–297). Oxbow Books.

Shaukat, S. S., Rao, T. A., & Khan, M. A. (2016). Impact of sample size on principal component analysis ordination of an environmental data set: Effects on eigenstructure. *Ekológia (Bratislava), 35*, 173–190.

Shillito, L. M. (2017). Multivocality and multiproxy approaches to the use of space: Lessons from 25 years of research at Catalhöyük. *World Archaeology, 49*, 237–259.

Small, A. (1969). Burghead. *Scottish Archaeological Forum, 1*, 61–68.

Smith, H. (1996). An investigation of site formation processes on a traditional Hebridean farmstead using environmental and geoarchaeological techniques. In D. Gilbertson, M. Kent, & J. Grattan (Eds.), *The outer Hebrides: The last 14,000 years* (pp. 195–206). Sheffield Academic Press.

Soil Survey of Scotland Staff. (1981). *Soil maps of Scotland at a scale of 1:250 000*. Macaulay Institute for Soil Research.

Stoops, G. (2021). *Guidelines for analysis and description of soil and regolith thin sections* (2nd ed.). Soil Science Society of America.

Stoops, G., Marcelino, V., & Mees, F. (Eds.). (2018). *Interpretation of micromorphological features of soils and regoliths* (2nd ed.). Elsevier.

Strachan, D., Sneddon, D., & Tipping, R. (2019). *Early medieval settlement in upland Perthshire: Excavations at Lair, Glen Shee, 2012–17.* Archaeopress.

Sulas, F., Bagge, M. S., Enevold, R., Harrault, L., Kristiansen, S. M., Ljungberg, T., Milek, K. B., Mikkelsen, P. H., Jensen, P. M., Orfanou, V., Out, W. A., Portillo, M., & Sindbæk, S. M. (2022). Revealing the invisible dead: Integrated bio-geoarchaeological profiling exposes human and animal remains in a seemingly 'empty' Viking-Age burial. *Journal of Archaeological Science, 141*, 105589.

University of Stirling. (2008). *Methods. Thin Section & Micromorphology,* University of Stirling. https://www.thin.stir.ac.uk/category/methods/

Weiner, S. (2010). *Microarchaeology: Beyond the visible archaeological record.* Cambridge University Press.

Wilson, C. A., Cresser, M. S., & Davidson, D. A. (2006). Sequential element extraction of soils from abandoned farms: An investigation of the partitioning of anthropogenic element inputs from historic land use. *Journal of Environmental Monitoring, 8*, 439–444.

Wilson, C. A., Davidson, D. A., & Cresser, M. S. (2005). An evaluation of multielement analysis of historic soil contamination to differentiate space use and former function in and around abandoned farms. *The Holocene, 15*, 1094–1099.

Wilson, C. A., Davidson, D. A., & Cresser, M. S. (2008). Multi-element soil analysis: An assessment of its potential as an aid to archaeological interpretation. *Journal of Archaeological Science, 35*, 412–424.

Wouters, B., Devos, Y., Vrydaghs, L., Ball, T., De Winter, N., & Reygel, P. (2019). An integrated micromorphological and phytolith study of urban soils and sediments from the Gallo-Roman town Atuatuca Tungrorum, Belgium. *Geoarchaeology, 34*, 448–466.

Young, H. W. (1891). Notes on the ramparts of Burghead, as revealed by recent excavations. *Proceedings of the Society of Antiquaries of Scotland, 25*, 435–447.

Young, H. W. (1893). Notes on further excavations at Burghead. *Proceedings of the Society of Antiquaries of Scotland, 27*, 86–91.

SUPPORTING INFORMATION

Additional supporting information can be found online in the Supporting Information section at the end of this article.